EEET ECOLOGICAL ENGINEERING & ENVIRONMENTAL TECHNOLOGY

Ecological Engineering & Environmental Technology, 2026, 27(3), 67–90
https://doi.org/10.12912/27197050/217648
ISSN 2719–7050, License CC-BY 4.0

Received: 2026.01.20
Accepted: 2026.02.20
Published: 2026.03.01

Enhancement of biogas production from Indonesian tofu industry liquid waste

Trifandi Lasalewo[1*], Iqbal Syaichurrozi[2]

[1] Department of Industrial Engineering, Universitas Negeri Gorontalo, Jl. Jend. Sudirman No.6, Kota Gorontalo, Gorontalo, 96128, Indonesia
[2] Department of Chemical Engineering, Faculty of Engineering, Universitas Sultan Ageng Tirtayasa, Cilegon, Banten, Indonesia
* Corresponding author's e-mail: trifandilasalewo@ung.ac.id

ABSTRACT

Tofu industry liquid waste (TILW) contains high organic content, so direct discharge into the environment is unacceptable. Thus, this waste is suitable to be processed to biogas via anaerobic digestion (AD). Biogas can be enhanced through trace element addition and the combination of AD with other methods. Therefore, this study aimed to evaluate the effect of $NiCl_2.6H_2O$ supplementation and microbial electrolysis cell integration (AD-MEC) on biogas production from TILW. Batch experiments were conducted with $NiCl_2.6H_2O$ concentrations of 0–8 mg/L. Then, the performance of AD and AD-MEC was compared. In the AD-MEC, the voltage was kept constant at 1.5 V. The results showed that AD-MEC with 2 mg/L $NiCl_2.6H_2O$ achieved the highest cumulative biogas yield of 550.82 mL/L and cumulative methane yield of 396.48 mL-CH_4/L. Due to the presence of MEC in AD at the same $NiCl_2.6H_2O$ dose (2 mg/L), total solid (TS) removal increased from 28.57% in AD to 37.50% in AD-MEC, while total suspended solid (TSS) and total dissolved solid (TDS) removals improved from 25.81% to 39.87% and from 31.14% to 34.93%, respectively. Despite requiring a small electrical input, AD-MEC generated a surplus energy of 3915.79 J, about 34% or 1.3 times higher than conventional AD. Therefore, AD-MEC with an addition of 2 mg/L $NiCl_2.6H_2O$ provided the optimal condition for TILW treatment by enhancing methane production, energy recovery, and pollutant removal.

Keywords: anaerobic digestion, microbial electrolysis cell, tofu industry liquid waste, trace element.

INTRODUCTION

The rapid expansion of agro-industrial activities has led to a significant increase in the generation of organic wastewaters, which poses considerable environmental challenges if not managed. Among these wastewaters is liquid waste from the tofu industry (TILW), which is characterized by elevated organic matter content (Huwaida et al., 2024). Untreated TILW discharge can cause oxygen depletion and eutrophication, highlighting the need for effective and sustainable treatment technologies (Rahmat et al., 2014). Anaerobic digestion (AD) has been recognized as an environmentally friendly and energy-efficient technology for treating high-strength organic wastewater while producing renewable energy in the form of biogas (Arifan et al., 2021). However, the performance of AD is often compromised by issues such as process instability, prolonged startup time, and inhibition due to unfavorable substrate characteristics, particularly nutrient imbalances and deficiencies in trace elements. Therefore, improving AD performance through appropriate inoculum selection and trace element supplementation has been widely proposed (Fermoso et al., 2009; Takashima et al., 2011). Rumen fluid, a rich source of diverse microbial communities including hydrolytic, acidogenic, acetogenic, and methanogenic microorganisms, has garnered interest as an inoculum source in AD systems. Studies indicate that the application of rumen inoculum can

significantly improve substrate degradation efficiency and promote the conversion of complex organic materials into methane, thereby optimizing biogas production (Ramadhani et al., 2025).

Trace elements are essential for the stability and metabolic activity of anaerobic microbes, including nickel (Ni), which plays a crucial role in supporting the methanogenic pathway. Ni is widely considered an essential micronutrient for methanogens because it directly participates in key enzymatic reactions during methane formation (Khan et al., 2021). When availability is too low, methanogenic activity is limited, and biogas production decreases, while excess Ni can cause toxic stress and disrupt the structure of microbial communities (Paulo et al., 2017). Therefore, determining the optimal Ni dose is crucial to maximizing biogas production while maintaining process stability. Recent advances in bioelectrochemical systems, particularly AD coupled with microbial electrolysis cells (AD-MEC), have shown promise in further improving biogas production (Wang et al., 2024). The integration of MEC in AD can improve electron transfer efficiency and promote direct interspecific electron transfer (DIET), thereby stimulating the methanogenic pathway and increasing methane yield (Syaichurrozi et al., 2024).

Although the role of nickel (Ni) as a catalytic trace metal in AD has been widely acknowledged, more recent evidence shows that its stimulatory effect is highly dependent on the applied dose, chemical speciation, and the nature of the substrate. Abdelsalam et al. (2015) reported that 1 mg/L $NiCl_2$ represented an optimal threshold in the digestion of livestock manure, significantly improving biogas and methane yields to 507.9 and 279.3 mL/g-VS, respectively. This enhancement was linked to better hydrolysis, consistent with the findings of Osazuwa. (2022) who observed a 34.4% reduction in total solids after Ni addition compared with only 1.2% in the control. In the digestion of *Phragmites australis* straw with cow dung as an inoculum, Tian et al. (2016) found that the optimum range of Ni^{2+} concentrations of 0.8–2.0 mg Ni/L, which improved the total biogas yield by more than 18% compared to the control. It was closely related to enzymatic activation, particularly increased dehydrogenase activity. In contrast, substrates prone to rapid acidification, such as molasses, required a higher Ni^{2+} dose of 2 mg/L to reduce volatile fatty acid (VFA) accumulation and stabilize pH, as demonstrated by Khan et al. (2021). Regarding metal bioavailability, Tsapekos et al. (2018) further demonstrated that Ni-salt ($NiCl_2.6H_2O$) of 5 mg/kg-VS supplemented with nitrilotriacetic acid (NTA) of 2 mg/L could match or exceed the performance of nickel nanoparticles in sewage sludge digestion, underscoring that chemical accessibility governs methanogenic efficiency.

Based on the information above, the addition of $NiCl_2.6H_2O$ to increase biogas production from TILW has not studied by others yet. Furthermore, comparative studies examining the impact of $NiCl_2.6H_2O$ supplementation in AD and AD-MEC processes for producing biogas from TILW are notably scarce. Therefore, this study is proposed with the aim of investigating the effect of $NiCl_2.6H_2O$ supplementation on increasing biogas production from TILW using rumen inoculum in both AD and AD-MEC processes. The new scientific result to be achieved is the optimum $NiCl_2.6H_2O$ dose in the AD and AD-MEC processes that convert TILW to biogas. The optimum $NiCl_2.6H_2O$ dose is determined based on the highest biogas yield, methane yield, and pollutant reduction. New things that need to be studied are the effects of variations in $NiCl_2.6H_2O$ concentrations on the profiles of biogas production, methane production, pH, volatile fatty acids (VFAs), and pollutant reduction during the AD and AD-MEC processes. Furthermore, the kinetic analysis is conducted to get a better understanding of the effect of $NiCl_2.6H_2O$ addition on the mechanisms during the processes. In addition, energy analysis is conducted to determine the feasibility of the presence of MEC in the AD process. The gap that will be filled by this research is the lack of information regarding the optimum $NiCl_2.6H_2O$ dose in increasing biogas production from TILW. It is hypothesized that appropriate Ni dosing will significantly enhance biogas and methane yields by stimulating key enzymatic pathways, with a more pronounced effect observed in the AD-MEC process due to enhanced DIET.

MATERIALS AND METHODS

Materials

The primary substrate used in this study was TILW collected from a tofu industry located in Sukmajaya Subdistrict, Jombang District, Cilegon City, Banten Province, Indonesia. Prior to use, the wastewater was homogenized to ensure a uniform composition throughout the experiments. Fresh rumen fluid was employed as the inoculum

and was obtained from a local slaughterhouse in Jombang District, Cilegon City, Banten Province, Indonesia. The authors determined the characteristics of TILW and inoculum (rumen fluid) using analytical methods. The liquid pH and VFAs were measured using a pH meter and the steam distillation method, respectively, with the detailed procedures shown in point 2.5.1. Then, total solid (TS) and total suspended solid (TSS) were measured using the gravimetric method with the detailed procedures shown in point 2.5.2. Furthermore, total dissolved solid (TDS) was calculated by the difference between TS and TSS (see point 2.5.2). The chemical oxygen demand (COD) was determined through closed reflux-spectrophotometry with the detailed procedures reported in previous studies (Khomariah et al., 2025; Syaichurrozi et al., 2025). The characteristics of the TILW and inoculum are presented in Table 1.

Experimental set-up

A batch AD digester was constructed using an Erlenmeyer flask with a total volume of 600 mL and a working volume of 500 mL. The digestion process was conducted using both AD and AD-MEC systems under batch conditions, with no influent or effluent flow during operation. For the AD-MEC system, the graphite carbon (black, purity of 99.9%) was used as the electrodes. Anode and cathode (placed with a distance of about 1.1 cm) were connected to the positive and negative poles of the direct current (DC) power supply. The voltage was adjusted to 1.5 V. Biogas produced during digestion was measured via the liquid displacement method. A silicone pipe was installed to facilitate gas sampling, while a liquid sampling port was located at the bottom of the digester for periodic liquid sampling. A detailed experimental setup for AD and AD-MEC is shown in Figure 1.

In this experimental setup, the conventional instrument for measuring biogas volume was applied, namely the liquid displacement method. In this method, a reversed measuring cylinder was filled with a saturated salt solution. As biogas was produced, it flew from the digester into the reversed measuring cylinder, displacing the salt solution in the reversed measuring cylinder. Changes in the level of the saturated salt solution in the reversed measuring cylinder were measured daily. Then, the daily biogas volume was calculated using a formula of $V_d = \frac{1}{4}\pi d^2 \Delta h$, where V_d is the daily biogas volume, d is the diameter of the reversed measuring cylinder, and Δh is the change in the level of the saturated salt solution in the reversed measuring cylinder.

Experimental design

The experimental design is summarized in Table 2. TILW and inoculum were mixed at a volumetric ratio of 80:20 (v/v). The initial pH of

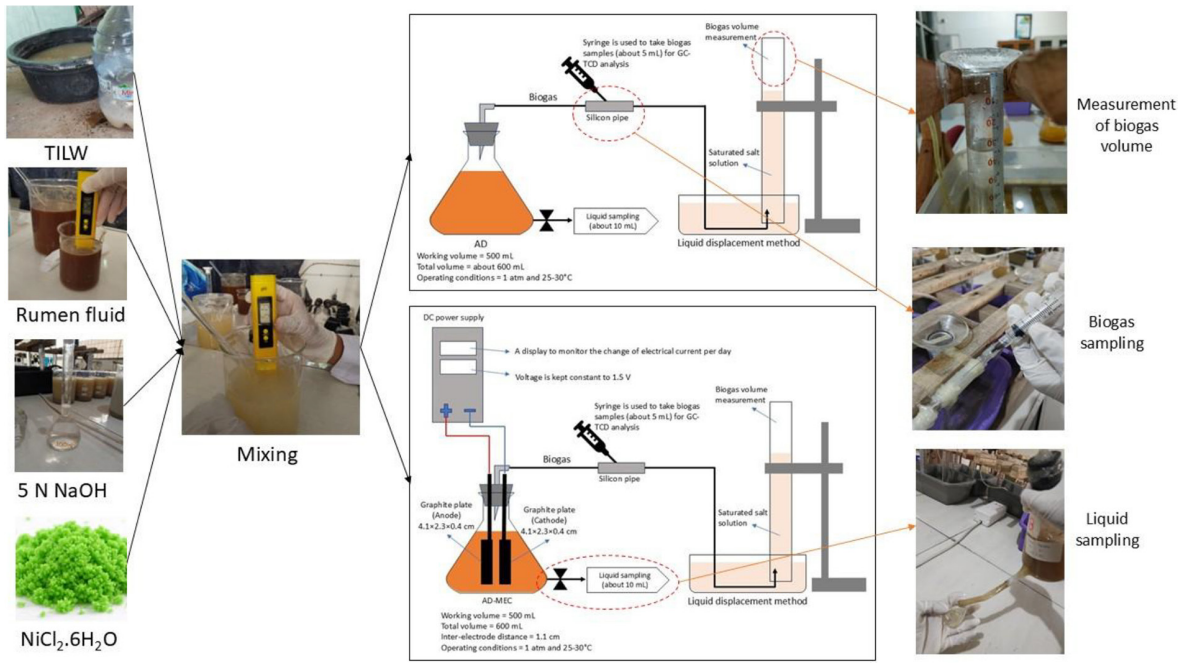

Figure 1. Experimental set-up of laboratory-scale process

Table 1. Characteristics of materials

Parameters	Units	Methods	TILW	Inoculum
pH	-	Using a digital pH meter	6.33	4.24–4.71
COD	mg-O_2/L	Closed reflux-spectrophotometry	5487.3	13266.7–20635.3
TS	mg-dry matter/L	Gravimetric method	8500	32000–46500
TSS	mg-dry matter/L	Gravimetric method	6000	8000–15000
TDS	mg-dry matter/L	Calculation (difference between TS and TSS)	2500	24000–31500
VFAs	mg-acetic acid/L	Steam distillation	1182.6	8056.5–8850.6

the mixture was adjusted to a pH of 7.0 using a 5 M NaOH solution. Nickel was supplemented in the form of $NiCl_2.6H_2O$ at concentrations of 0, 2, 4, 6, and 8 mg/L for the AD system. Based on the optimum $NiCl_2.6H_2O$ concentration obtained from the AD experiments, selected doses of 2 and 4 mg/L were further applied in the AD-MEC system. All digesters were operated in batch mode under ambient conditions (1 atm and 25–30 °C).

Experimental procedure

Stage 1 (AD process)

TILW and inoculum were mixed at a volumetric ratio of 80:20 (v/v). The $NiCl_2.6H_2O$ was added with concentrations of 0, 2, 4, 6, and 8 mg/L. Then, the initial pH was adjusted to 7.0 using a 5 N NaOH solution. To maintain anaerobic conditions, the digesters were tightly sealed with rubber stoppers and wrapped with aluminium foil to prevent light interference that could negatively affect methanogenic activity.

Stage 2 (AD vs AD-MEC processes)

TILW and inoculum were mixed at a volumetric ratio of 80:20 (v/v). The $NiCl_2.6H_2O$ was added with concentrations of 2 and 4 mg/L (optimum concentrations based on Stage 1). Then, the initial pH was adjusted to 7.0 using a 5 N NaOH solution. Anode and cathode (placed with a distance of about 1.1 cm) were connected to the positive and negative poles of the direct current (DC) power supply. The voltage was adjusted to 1.5 V. To maintain anaerobic conditions, the digesters were tightly sealed with rubber stoppers and wrapped with aluminum foil to prevent light interference that could negatively affect methanogenic activity.

Measurements and sampling in stages 1 and 2

The AD and AD-MEC processes were carried out for 15 days. Biogas volume was measured daily using the liquid displacement method, and the cumulative biogas volume was calculated by summing the daily measurements. The changes in electrical current during the AD-MEC process were monitored using a digital multimeter. Gas samples of 5 mL were withdrawn every three days using a syringe. Then, they were transferred into vacuum tubes and analyzed for gas composition (CH_4 and CO_2) using gas chromatography equipped with a thermal conductivity detector (GC-TCD). Before liquid sampling was conducted, the digesters were shaken manually to ensure homogeneity. Liquid samples (approximately 10 mL) were withdrawn every three days (days 3, 6, 9, 12, and 15). Then, the pH and VFA concentration of all liquid samples were measured using a

Table 2. Experimental design

Digester	TILW volume (mL)	Inoculum volume (mL)	Process	$NiCl_2.6H_2O$ (mg/L)
1	400	100	AD	0
2	400	100	AD	2
3	400	100	AD	4
4	400	100	AD	6
5	400	100	AD	8
6	400	100	AD-MEC	2
7	400	100	AD-MEC	4

digital pH meter and the steam distillation method, respectively. At the end of the process (on day 15), the digestates in the digesters were collected for TS, TSS, and TDS analyses.

Analyses

pH and VFA

The pH of the liquid was measured using a calibrated digital pH meter. VFAs were determined using a steam distillation method following the procedure reported by Syaichurrozi et al. (2024) with minor modifications. About 2 mL of the liquid sample was diluted to 100 mL with deionized water. Then, it was added with 100 mL of deionized water, acidified with 5 mL of 50% H_2SO_4, and distilled until approximately 150 mL of distillate was collected. The distillate was then titrated with 0.05 N NaOH using phenolphthalein as an indicator, and the VFA concentration in the sample was calculated using Equation 1.

$$\text{VFAs}\left(\frac{\text{mg}_{\text{acetic acid}}}{\text{L}}\right) = \frac{\text{V}_{\text{NaOH}} \times \text{N}_{\text{NaOH}} \times \times \text{MW}_{\text{acetic acid}} \times 1000}{\text{V}_{\text{sample}} \times \text{F}_{\text{recovery}}} \quad (1)$$

where: V_{NaOH} is the volume of NaOH solution (mL), N_{NaOH} is the normality of NaOH solution (mol/L), $MW_{acetic\ acid}$ is the molecular weight of acetic acid (g/mol), V_{sample} is the volume of the sample (mL), $F_{recovery}$ is the factor of recovery.

In the AD and AD-MEC processes, the initial pH was adjusted by adding 5 N NaOH solution and measured using a digital pH meter. During the process, the pH of samples on days 3, 6, 9, 12, and 15 was detected using a digital pH meter. The initial VFA concentration was calculated using Equation 2. During the process, the VFA concentration of samples on days 3, 6, 9, 12, and 15 was determined using steam distillation.

$$VFAs_{initial} = \frac{(VFAs_{TILW} \times volume_{TILW}) + (VFAs_{inoculum} \times volume_{inoculum})}{volume_{TILW} + volume_{inoculum}} \quad (2)$$

TS, TSS, and TDS

TS and TSS were determined by following the gravimetric methods described by Syaichurrozi et al. (2024). For TS analysis, a known volume of 10 mL of liquid sample was placed in a pre-dried and pre-weighed crucible. Then it was dried in an oven at 110 °C until a constant weight was achieved. The TS concentration was calculated using Equation 3.

$$TS\left(\frac{mg}{L}\right) = \frac{w_2 - w_1}{Sample\ volume} \quad (3)$$

where: w_1 is the weight of the empty crucible, $w_2$is the weight of the empty crucible with the dried solid.

TSS was determined by filtering 20 mL of the sample through pre-dried and pre-weighed Whatman No. 42 filter paper, followed by oven drying at 110 °C until a constant weight was obtained. The TSS concentration was calculated using Equation 4.

$$TSS\left(\frac{mg}{L}\right) = \frac{w_b - w_a}{Sample\ volume} \quad (4)$$

where: w_a is the weight of the empty Whatman No. 42 filter paper, w_b is the weight of the Whatman filter paper with the dried solid.

The total dissolved solids (TDS) concentration was calculated as the difference between TS and TSS using Equation 5.

$$TDS\left(\frac{mg}{L}\right) = TS\left(\frac{mg}{L}\right) - TSS\left(\frac{mg}{L}\right) \quad (5)$$

In the AD and AD-MEC processes, the initial TS, TSS, and TDS were calculated using Equation 6, 7, and 8.

$$TS_{initial} = \frac{(TS_{TILW} \times volume_{TILW}) + (TS_{inoculum} \times volume_{inoculum})}{volume_{TILW} + volume_{inoculum}} \quad (6)$$

$$TSS_{initial} = \frac{(TSS_{TILW} \times volume_{TILW}) + (TSS_{inoculum} \times volume_{inoculum})}{volume_{TILW} + volume_{inoculum}} \quad (7)$$

$$TDS_{initial} = \frac{(TDS_{TILW} \times volume_{TILW}) + (TDS_{inoculum} \times volume_{inoculum})}{volume_{TILW} + volume_{inoculum}} \quad (8)$$

Furthermore, the final TS, TSS, and TDS on day 15 were measured through the detailed procedures above. After that, the TS, TSS, and TDS removal were calculated using Equation 9, 10, and 11.

$$\text{TS removal} = \frac{\text{TS}_{\text{initial}} - \text{TS}_{\text{final}}}{\text{TS}_{\text{initial}}} \times 100\% \quad (9)$$

$$\text{TSS removal} = \frac{\text{TSS}_{\text{initial}} - \text{TSS}_{\text{final}}}{\text{TSS}_{\text{initial}}} \times 100\% \quad (10)$$

$$\text{TDS removal} = \frac{\text{TDS}_{\text{initial}} - \text{TDS}_{\text{final}}}{\text{TDS}_{\text{initial}}} \times 100\% \quad (11)$$

Biogas yield

In the AD and AD-MEC processes, the biogas volume measurement was conducted daily for 15 days. Biogas volume was quantified using the liquid displacement method by following the procedure described by Syaichurrozi et al. (2024). When biogas was generated in the digester, it flew into the reversed measuring cylinder, displacing the salt solution in the reversed measuring cylinder. Changes in the level of the saturated salt solution in the reversed measuring cylinder were measured daily. Then, the biogas volume was calculated using a formula of $V_d = \frac{1}{4}\pi d^2 \Delta h$, where V_d is the daily biogas volume, d is the diameter of the reversed measuring cylinder, and Δh is the change in the level of the saturated salt solution in the reversed measuring cylinder.

Figure 2 illustrates the biogas volume measurement. For example, on day 1, the change in the level was Δh_1, so the biogas volume on day 1 was $V_{d1} = \frac{1}{4}\pi d^2 \Delta h_1$. Furthermore, on day 2, the change in the level was Δh_2 so the biogas volume on day 1 was $V_{d2} = \frac{1}{4}\pi d^2 \Delta h_2$. The daily biogas volume measurement was conducted per day for 15 days. Then, the cumulative biogas volume was calculated by summing the daily biogas volumes. For example, the cumulative biogas volume on day 2 was the sum of $V_{d0} + V_{d1} + V_{d2}$. For the generalization of the results, biogas volume (mL) was converted to biogas yield (mL/L). Biogas yield (mL/L) was calculated by dividing the biogas (mL) by the volume of waste processed (0.4 L, see Table 2).

Methane content and methane yield

Methane (CH_4) and carbon dioxide (CO_2) contents in biogas were analyzed using gas chromatography-thermal conductivity detection (GC-TCD). The presence of air in the headspace might influence the results of the GC-TCD. Hence, the CH_4 content was recalculated via Equation 12 (Khomariah et al., 2025; Syaichurrozi et al., 2025).

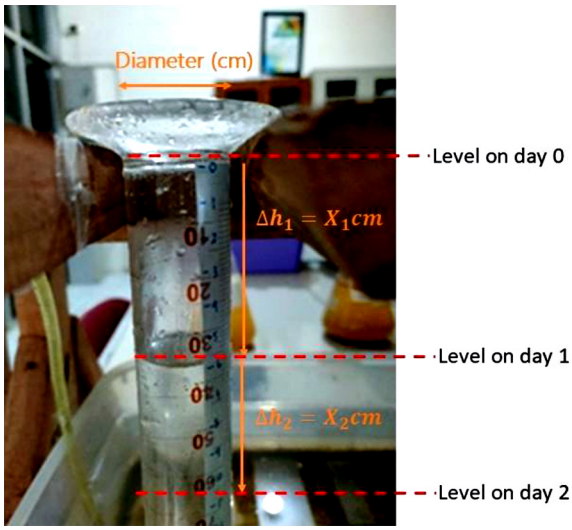

Figure 2. Biogas volume measurement

$$\%\text{CH}_4 = \frac{\%\text{CH}_{4,\text{GC-TCD}}}{\%\text{CO}_{2,\text{GC-TCD}} + \\ +\%\text{CH}_{4,\text{GC-TCD}}} \times 100\% \quad (12)$$

Based on the profiles of daily biogas volume during AD and AD-MEC, the biogas sample on day 3 was chosen to be analyzed for methane content through GC-TCD. It was because the most biogas volume was generated in days 1-3. Furthermore, the methane yield was calculated via Equation 13.

$$\text{Methane yield} = \text{Biogas yield} \times \\ \times \text{methane content} \quad (13)$$

Electrical current measurement

The daily changes in electrical current during the AD-MEC process were monitored using a digital multimeter.

Kinetics

Biogas production kinetics were evaluated using the modified Gompertz model, which includes three key parameters, namely maximum biogas production potential P_m, maximum production rate μ, and lag phase duration λ. This model was selected because it effectively describes cumulative biogas production in batch AD systems, where these parameters are closely associated with microbial growth and activity (Alharbi and Alkathami, 2024; Zwietering et al., 1990). The kinetic expression is presented in Equation 14, assuming that batch biogas

production follows microbial growth behavior. Parameter estimation was performed by minimizing the sum of squared errors (SSE) between experimental and predicted data (Equation 15). In addition, the goodness of fit of the model was evaluated using the coefficient of determination (R^2), which was calculated using Microsoft Excel, as defined in Equation 16.

$$P_t = P_m . exp\left\{-exp\left[\frac{\mu . e}{P_m}(\lambda - t) + 1\right]\right\} \quad (14)$$

$$SSE = \sum_{i=1}^{n}\left(P_i - \hat{P}_i\right)^2 \quad (15)$$

$$R^2 = 1 - \frac{\sum_{i=1}^{n}\left(P_i - \hat{P}_i\right)^2}{\sum_{i=1}^{n}(P_i - \bar{P})^2} \quad (16)$$

where: P_t is the cumulative biogas production at time t (mL/L), P_m is the maximum biogas production potential (mL/L), μ is the maximum production rate (mL/L/d), λ is the lag phase duration (days), e is Euler's number (2.71828), and t is the digestion time (days). P_i, $\hat{P}_i$, and $\bar{P}$ represent the experimental data (mL/L), the modeled data (mL/L), and the mean of the experimental data (mL/L), respectively.

Energy analysis

In this study, the applied voltage was maintained constant at 1.5 V throughout the operation. However, changes in liquid conductivity during the process led to fluctuations in the measured electrical current. The energy potential of the produced biogas was then evaluated through an energy analysis following the approach proposed by Syaichurrozi et al. (2024). This analysis was performed to determine the feasibility of the AD-MEC system in treating TILW. The input energy was estimated using Equation 17.

$$Input\ energy\ (J) = Voltage\ (V) \times \times Current\ (A) \times Time\ (s) \quad (17)$$

Both AD and AD-MEC processes generate methane, which can be converted into useful energy through combustion. The energy output from methane production was estimated using Equation 18.

$$Output\ energy\ (J) = = \frac{\left[68\% \times 817{,}970\left(\frac{J}{mol}\right) \times Methane\ volume\ (L)\right]}{22.4\left(\frac{L}{mol}\right)} \quad (18)$$

The surplus energy was then determined as the difference between output and input energy, as expressed in Equation 19.

$$Surplus\ energy\ (J) = Output\ Energy\ (J) - Input\ Energy\ (J) \quad (19)$$

The illustration of experiments, measurements, and analyses is presented in Figure 3.

RESULTS AND DISCUSSION

AD process

Biogas production and methane content

The daily biogas production, as seen in Figure 4(a) and Table 3, shows that the addition of $NiCl_2.6H_2O$ affected the initial rate of biogas formation. The highest daily production was recorded on day 2, especially at a dose of 4 mg/L $NiCl_2.6H_2O$ with a volume of 161.55 mL/L, followed by 2 mg/L $NiCl_2.6H_2O$ with a volume of 150.78 mL/L, 6 mg/L $NiCl_2.6H_2O$ with a volume of 146.17 mL/L, 0 mg/L $NiCl_2.6H_2O$ (control) with a volume of 109.24 mL/L, and 8 mg/L $NiCl_2.6H_2O$ with a volume of 46.15 mL/L on day 3. This highest biogas peak indicates that Ni acts as an essential trace element that accelerates the activation of key enzymes such as Ni-dependent hydrogenase and methyl-coenzyme M reductase (MCR), thus accelerating the conversion of organic compounds into methane precursors during the methanogenesis phase and resulting in a short adaptation phase and a more spontaneous conversion of the substrate to biogas (Tian et al., 2016). After the 3rd day, daily biogas production decreased drastically at all doses, even approaching zero on days 4–6 at doses of 0, 6, and 8 mg/L $NiCl_2.6H_2O$, indicating the emergence of an inhibitory effect. This effect occurs because excessive Ni^{2+} concentrations no longer act as a micronutrient but instead become an inhibitor. At higher levels, Ni^{2+} can exert toxic stress on sensitive microbial groups, particularly acetoclastic methanogens, and can disrupt cellular osmotic and ionic balance, ultimately impairing

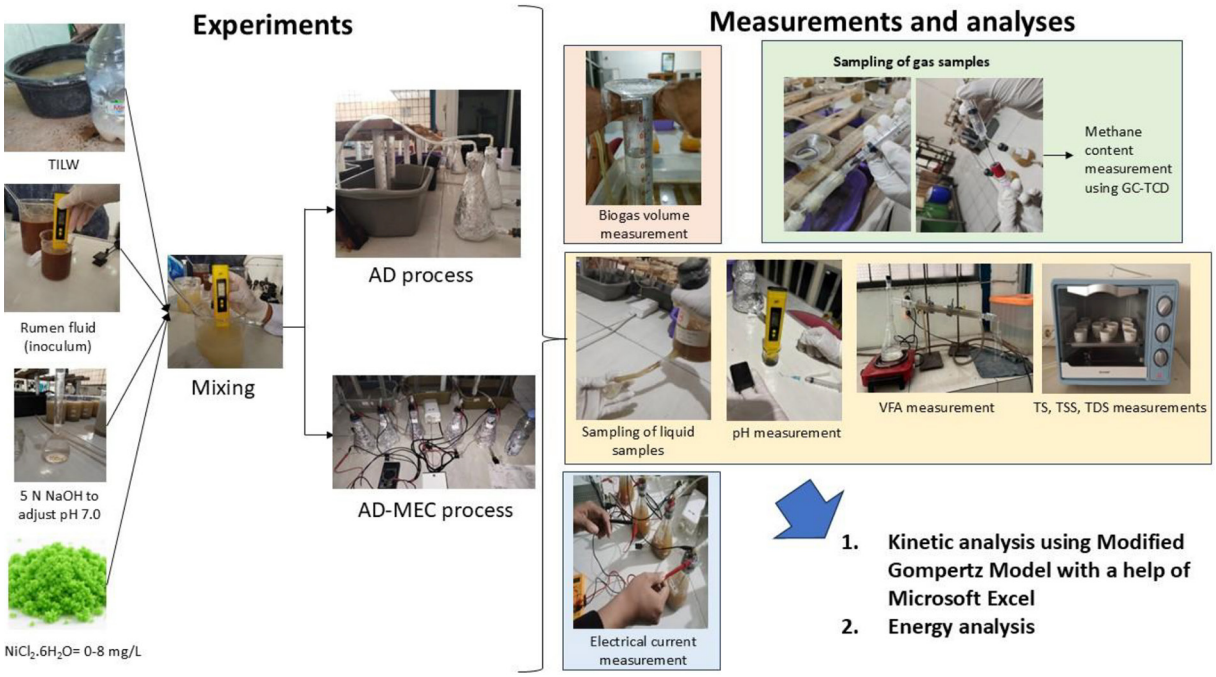

Figure 3. Illustration of experiments, measurements, and analyses

their metabolic activity and methane production (Matheri and Belaid, 2016). Then, the presence of Cl^- in high concentrations is thought to increase the ionic pressure of the medium and exacerbate microbial stress, where in easily acidified substrates, it causes VFA accumulation and partial inhibition of methanogenesis. Chloride ions (Cl^-), although not directly catalytic, contribute to ionic strength. At high concentrations, $NiCl_2.6H_2O$ can exacerbate osmotic stress, amplifying Ni toxicity rather than enhancing bioavailability. The 4 mg/L $NiCl_2.6H_2O$ dose showed a more stable daily profile with a significant peak on day 2 with a daily biogas yield of 161.55 mL/L, indicating a better balance between enzymatic stimulation and microbial tolerance.

In cumulative biogas production as seen in Figure 4(b) and Table 3, the dose of 4 mg/L $NiCl_2.6H_2O$ produced the highest total biogas yield of 350.80 mL/L compared to other doses, followed by 2 mg/L $NiCl_2.6H_2O$ with a total volume of 315.41 mL/L, 6 mg/L $NiCl_2.6H_2O$ with a total volume of 304.64 mL/L, 0 mg/L $NiCl_2.6H_2O$ (control) with a total volume of 167.71 mL/L, and 8 mg/L $NiCl_2.6H_2O$ with a total volume of 124.63 mL/L. The superiority of the 4 mg/L $NiCl_2.6H_2O$ reflects the optimum condition where Ni is available enough to meet the metabolic needs of microorganisms without causing toxic effects or ionic interference, so that the methanogenesis process can last longer and be more stable. This finding is consistent with Tsapekos et al. (2018), who emphasized that the effectiveness of Ni is determined more by its bioavailability and proper dosage than by its mere presence and that the more pronounced impact on methanogenesis than can be attributed to the fact that nickel is more important for the growth of archaea than for bacterial species, as it contributes to maintaining cell membranes and increasing structural stability.

At a dose of 2 mg/L $NiCl_2.6H_2O$, the system experienced nutrient limitation, where the reaction rate is limited by the lack of metal cofactors, even though the substrate is still available, in line with the trace element limitation theory presented by Khan et al. (2021). At a dose of 6 mg/L $NiCl_2.6H_2O$, although initial production was high, it was thought to be due to the accumulation of Ni^{2+} and Cl^-, which accelerated the occurrence of partial inhibition, which caused the cumulative contribution to be lower than that of 4 mg/L $NiCl_2.6H_2O$. Meanwhile, a dose of 8 mg/L $NiCl_2.6H_2O$ showed the most obvious negative effect, which was lower than the control (0 mg/L $NiCl_2.6H_2O$), which was logically related to metal toxicity and disruption of microbial balance, so that both the daily and cumulative biogas yields were the lowest. At a concentration of 8 mg/L $NiCl_2.6H_2O$, Ni ions no longer function as nutrients, but rather as competitive inhibitors that

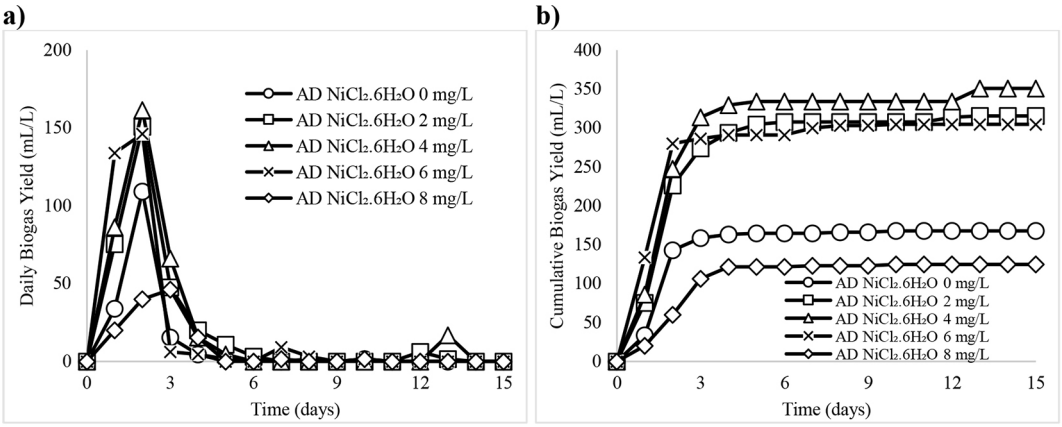

Figure 4. (a) Daily biogas yield, (b) cumulative biogas yield in the AD process

Table 3. Numerical results of daily and cumulative biogas yields during the AD process at various $NiCl_2.6H_2O$ doses of 0-8 mg/L

Day	Daily biogas yield (mL/L)					Cumulative biogas yield (mL/L)				
	AD 0 mg/L	AD 2 mg/L	AD 4 mg/L	AD 6 mg/L	AD 8 mg/L	AD 0 mg/L	AD 2 mg/L	AD 4 mg/L	AD 6 mg/L	AD 8 mg/L
0	0.00	0.00	0.00	0.00	0.00	0.00	0.00	0.00	0.00	0.00
1	33.85	75.39	86.16	133.86	20.00	33.85	75.39	86.16	133.86	20.00
2	109.24	150.78	161.55	146.17	40.00	143.09	226.17	247.71	280.03	60.01
3	15.39	47.70	66.16	6.15	46.16	158.48	273.87	313.87	286.18	106.16
4	4.62	20.00	15.39	4.62	15.39	163.09	293.87	329.26	290.80	121.55
5	1.54	10.77	4.62	0.00	0.00	164.63	304.64	333.88	290.80	121.55
6	0.00	3.08	0.00	0.00	0.00	164.63	307.72	333.88	290.80	121.55
7	0.00	0.00	0.00	9.23	1.54	164.63	307.72	333.88	300.03	123.09
8	1.54	0.00	0.00	3.08	0.00	166.17	307.72	333.88	303.10	123.09
9	0.00	0.00	0.00	0.00	0.00	166.17	307.72	333.88	303.10	123.09
10	1.54	0.00	0.00	1.54	1.54	167.71	307.72	333.88	304.64	124.63
11	0.00	0.00	0.00	0.00	0.00	167.71	307.72	333.88	304.64	124.63
12	0.00	6.15	0.00	0.00	0.00	167.71	313.87	333.88	304.64	124.63
13	0.00	1.54	16.92	0.00	0.00	167.71	315.41	350.80	304.64	124.63
14	0.00	0.00	0.00	0.00	0.00	167.71	315.41	350.80	304.64	124.63
15	0.00	0.00	0.00	0.00	0.00	167.71	315.41	350.80	304.64	124.63

displace other essential metals in the thiol group of the enzyme and damage the integrity of the bacterial cell wall. This systemic failure at a dose of 8 mg/L $NiCl_2.6H_2O$ confirms that the tolerance limit of methanogens to nickel is very narrow, and even a small excess dose above the threshold of 6 mg/L will trigger a fatal crash process for biogas formation (Matheri and Belaid, 2016). Overall, these data confirm that Ni in the form of $NiCl_2.6H_2O$ functions as a crucial enzymatic cofactor in AD, but is only effective within a narrow dose range. Excess Ni and Cl^- actually shift the system from a bio-stimulatory state to an inhibitory state.

The methane content in biogas was analyzed and shown in Table 4. Furthermore, the daily and cumulative methane yields (mL-CH_4/L) were calculated and shown in Figure 5(a) and Figure 5(b), respectively. The numerical results are shown in Table 5.

The daily methane yield profile, as shown in Figure 5(a) and Table 5, indicates that the addition of $NiCl_2.6H_2O$ accelerated and enhanced methane formation in the early phase of anaerobic digestion with a highly dose-dependent response. Based on the daily methane yield data, the dose of 4 mg/L $NiCl_2.6H_2O$ showed the highest

Table 4. Methane concentration in biogas in the AD process

Sample	CH_4 content (%)*
AD $NiCl_2.6H_2O$ 0 mg/L	75.9
AD $NiCl_2.6H_2O$ 2 mg/L	83.9
AD $NiCl_2.6H_2O$ 4 mg/L	84.0
AD $NiCl_2.6H_2O$ 6 mg/L	81.9
AD $NiCl_2.6H_2O$ 8 mg/L	82.0

Note: *measured on day 3 and assumed as the average value.

performance in the early phase of digestion, with the highest daily methane yield peak achieved on day 2 at 135.78 mL-CH_4/L, followed by 2 mg/L $NiCl_2.6H_2O$ at 126.56 mL-CH_4/L, and then 6 mg/L $NiCl_2.6H_2O$ at 119.71 mL-CH_4/L. The $NiCl_2.6H_2O$ concentration of 4 mg/L was the most effective dose in accelerating the initial methanogenesis rate. This shows that at 4 mg/L, Ni^{2+} availability is at an optimal level to activate methanogenic redox enzymes without causing toxic stress or ionic balance disturbances, in addition to showing an acceleration of the methanogenesis phase due to the role of Ni as an important cofactor for key enzymes such as methyl-coenzyme M reductase (MCR) and Ni-dependent hydrogenase that accelerate the conversion of acetate and H_2/CO_2 to CH_4. MCR is a key enzyme containing the cofactor F_{430} (nickel porphyrinoid), which is responsible for the final stage of methane formation. These co-factors in enzymes decompose larger organics to smaller molecules (Matheri and Belaid, 2016; Neubeck et al., 2016; Tian et al., 2016). Compared to the 0 mg/L (control), which only produced 82.90 mL-CH_4/L on day 2, indicating that without the Ni cofactor, the MCR enzyme cannot function efficiently, the system with Ni showed a much stronger metabolic activation. At a dose of 6 mg/L $NiCl_2.6H_2O$, although an initial spike still occurred, the daily methane yield rapidly declined after day 2 and became unstable. Similarly, at a dose of 2 mg/L $NiCl_2.6H_2O$, the decline occurred after day 4, indicating that the initial overstimulation was not followed by sustained microbial activity. At a high dose of 8 mg/L $NiCl_2.6H_2O$, the daily methane yield was much lower from the start and rapidly declined, indicating an inhibitory effect. Excess Ni^{2+} can cause toxic stress in sensitive methanogens, particularly acetoclastic methanogens, and disrupt the microbial community balance after the readily degradable substrate fraction is depleted (Matheri and Belaid, 2016; Tian et al., 2016).

Cumulative methane yield is shown in Figure 5(b) and Table 5, where 4 mg/L $NiCl_2.6H_2O$ generated the highest total methane yield at 294.84 mL-CH_4/L, followed by 2 mg/L $NiCl_2.6H_2O$ at 264.74 mL-CH_4/L, and then 6 mg/L $NiCl_2.6H_2O$ at 249.51 mL-CH_4/L. The dose of 4 mg/L $NiCl_2.6H_2O$ was superior both daily and cumulatively, indicating that this dose not only accelerated the initial reaction but was also able to maintain the conversion of VFAs to methane more consistently throughout the digestion time. Then followed by a dose of 2 mg/L $NiCl_2.6H_2O$, which showed that this dose was very stable but slightly slower in utilizing the rapidly degraded substrate fraction. Meanwhile, the dose of 6 mg/L $NiCl_2.6H_2O$ was even smaller than the dose of 2 mg/L $NiCl_2.6H_2O$ due to further disturbances in the methanogenic community, due to ionic stress, and the possibility of suspected syntrophic imbalance after the

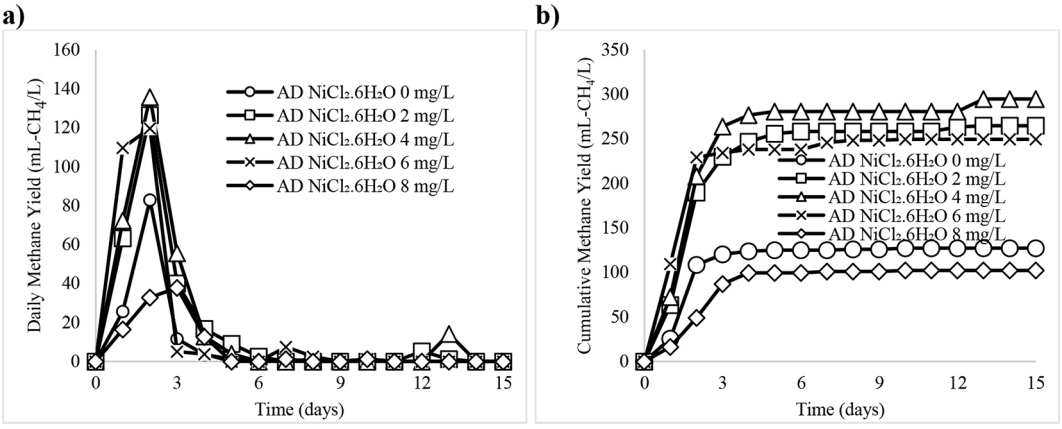

Figure 5. (a) Daily methane yield, (b) cumulative methane yield in the AD process

Table 5. Numerical results of daily and cumulative methane yields during the AD process at various $NiCl_2.6H_2O$ doses of 0–8 mg/L

Day	Daily methane yield (mL-CH_4/L)					Cumulative methane yield (mL-CH_4/L)				
	0 mg/L	2 mg/L	4 mg/L	6 mg/L	8 mg/L	0 mg/L	2 mg/L	4 mg/L	6 mg/L	8 mg/L
0	0.00	0.00	0.00	0.00	0.00	0.00	0.00	0.00	0.00	0.00
1	25.69	63.28	72.42	109.63	16.40	25.69	63.28	72.42	109.63	16.40
2	82.90	126.56	135.78	119.71	32.81	108.58	189.84	208.20	229.34	49.21
3	11.68	40.03	55.61	5.04	37.86	120.26	229.88	263.80	234.38	87.07
4	3.50	16.79	12.93	3.78	12.62	123.76	246.66	276.74	238.17	99.69
5	1.17	9.04	3.88	0.00	0.00	124.93	255.70	280.62	238.17	99.69
6	0.00	2.58	0.00	0.00	0.00	124.93	258.29	280.62	238.17	99.69
7	0.00	0.00	0.00	7.56	1.26	124.93	258.29	280.62	245.73	100.95
8	1.17	0.00	0.00	2.52	0.00	126.10	258.29	280.62	248.25	100.95
9	0.00	0.00	0.00	0.00	0.00	126.10	258.29	280.62	248.25	100.95
10	1.17	0.00	0.00	1.26	1.26	127.26	258.29	280.62	249.51	102.21
11	0.00	0.00	0.00	0.00	0.00	127.26	258.29	280.62	249.51	102.21
12	0.00	5.17	0.00	0.00	0.00	127.26	263.45	280.62	249.51	102.21
13	0.00	1.29	14.22	0.00	0.00	127.26	264.74	294.84	249.51	102.21
14	0.00	0.00	0.00	0.00	0.00	127.26	264.74	294.84	249.51	102.21
15	0.00	0.00	0.00	0.00	0.00	127.26	264.74	294.84	249.51	102.21

initial phase. The control without Ni or a dose of 0 mg/L produced a much lower cumulative methane of 127.26 mL-CH_4/L, indicating that the absence of trace metal $NiCl_2.6H_2O$ limits methanogenesis capacity. Meanwhile, at a higher dose of 8 mg/L $NiCl_2.6H_2O$, the lowest result was only 102.21 mL-CH_4/L, indicating that at this concentration, Ni^{2+} has approached the biological tolerance threshold or toxicity limit for TILW-degrading bacteria, causing disruption of the enzyme's thiol group (Matheri and Belaid, 2016; Khan et al., 2021). These results confirm that $NiCl_2.6H_2O$ functions as a critical trace metal in AD with a key role in the activation of methanogenic enzymes and trace metal additives that can enhance organic matter degradation and increase methane production yields, but are only effective at certain doses (Osazuwa, 2022). Doses that are too low limit enzyme activity, while doses that are too high accelerate microbial stress and reduce long-term efficiency. The data above can be concluded that the optimum $NiCl_2.6H_2O$ dose is 4 mg/L because it is able to provide the highest daily yield as well as maximum methane accumulation.

Based on Table 4, the addition of $NiCl_2.6H_2O$ not only increased the methane yield but also improved the biogas quality by increasing the CH_4 content. The AD system without $NiCl_2.6H_2O$ addition (0 mg/L) produced the lowest CH_4 content of 75.9%, which was consistent with the lowest daily and cumulative methane yields, indicating that trace metal limitations limited methanogen activity and caused some carbon to be converted to CO_2 or intermediate compounds. The doses of 2 and 4 mg/L $NiCl_2.6H_2O$ significantly increased the CH_4 content to 83.9% and 84.0%, respectively, directly correlated with the high daily methane yield in the initial phase from days 1 to 3 and the stable methane accumulation throughout the digestion period. This increase in the CH_4 content indicates that Ni at medium doses effectively activates the methanogenesis pathway, particularly in hydrogenotrophic and acetoclastic methanogens, resulting in a greater proportion of electrons ending up as CH_4 than CO_2. Interestingly, at a dose of 6 mg/L $NiCl_2.6H_2O$, although the cumulative methane yield was high, the CH_4 fraction actually decreased slightly to 81.9%, which explains why the very high daily methane yield spike on days 1 and 2 did not fully continue proportionally in the long term. Higher Ni doses accelerated organic decomposition and total gas formation, but also increased the CO_2 fraction due to a temporary imbalance between acidogenesis and methanogenesis, as well as potential stress on methanogens that reduced the efficiency of electron conversion to CH_4. This phenomenon is consistent with the low daily methane yield after

the initial phase at a dose of 6 mg/L $NiCl_2.6H_2O$. At a dose of 8 mg/L $NiCl_2.6H_2O$, the CH_4 concentration of 82.0% was relatively high, but the methane yield remained the lowest, indicating that gas quality was unable to compensate for the decrease in quantity due to microbial inhibition. These data confirm that high CH_4 content should be interpreted in conjunction with methane yield, as the CH_4 fraction reflects the efficiency of the methanogenesis pathway, while yield reflects the sustainability and total capacity of the system. The combination of the two indicates that 4 mg/L $NiCl_2.6H_2O$ provided an optimal balance between methane quantity and quality.

Liquid pH and volatile fatty acids (VFAs)

The liquid pH profiles in Figure 6(a) and Table 6 show the balance between the formation and consumption of intermediate products during AD of TILW. In all variations, the initial pH was in the neutral range of 7.00–7.05, then decreased sharply until the 3rd day, namely 6.54–6.61. Impressively, the addition of 6 mg/L $NiCl_2.6H_2O$ showed the most significant pH recovery, with the pH value rising to 6.94 on day 15, while the other treatments tended to continue decreasing. This pattern suggests that at this concentration, Ni not only acts as an enzyme cofactor but also helps stabilize the process dynamics, allowing the rate of VFA consumption by methanogens to catch up with and even balance their rate of acid formation. Meanwhile, Cl^- ions at intermediate concentrations contribute to osmotic stability and ion transport across membranes, supporting the resilience of methanogenic cells to acid fluctuations. At lower $NiCl_2.6H_2O$ doses of 0–4 mg/L, the VFA consumption capacity was not strong enough to withstand the decrease in pH, whereas at 8 mg/L $NiCl_2.6H_2O$, early indications of ionic stress began to appear, so that pH recovery was limited.

Analysis of VFA concentrations revealed a dynamic inverse relationship to pH, as seen in Figure 6(b) and Table 6. Theoretically, a decrease in pH is correlated with an increase in VFAs (Syaichurrozi et al., 2024). The data shows that 6 mg/L $NiCl_2.6H_2O$ recorded the highest VFA accumulation of 4781.35 mg-acetic acid/L as well as the highest pH. A dose of 6 mg/L $NiCl_2.6H_2O$ might stimulate the rate of substrate hydrolysis and acidogenesis (VFA formation) much faster than the rate of its conversion to methane. Then, it was followed by the 0 mg/L (control), 8 mg/L, 2 mg/L, and 4 mg/L $NiCl_2.6H_2O$. The high VFA concentration at a dose of 6 mg/L $NiCl_2.6H_2O$ shows very high hydrolysis and acidogenesis efficiency, where Ni increases fermentative microbial activity and electron transfer between microbial populations, resulting in intensive formation of acetic, butyric, and other volatile acids. However, unlike the control, this system did not experience excessive acidification because VFA consumption by methanogens was also active, as evidenced by the increase in pH in the final phase. Meanwhile, in the control without Ni, the high accumulation of VFAs was not offset by further conversion due to limited methanogen kinetics, resulting in a lower pH and weak system stability. The relatively low levels of VFAs at $NiCl_2.6H_2O$ doses of 2–4 mg/L indicate that acid production and consumption occur at comparable rates, reflecting that methanogens remain metabolically active and continue to convert these intermediates to methane (Khan et al., 2021; Xu et al., 2020). Within this range,

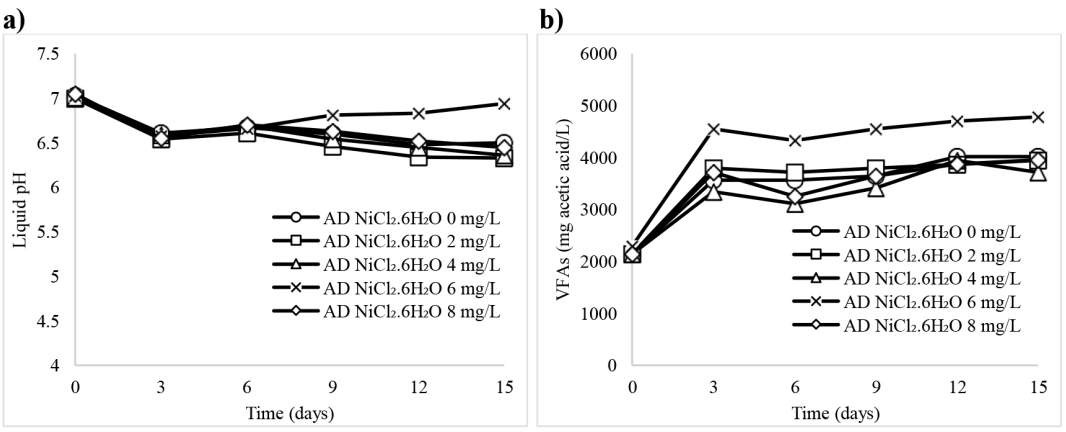

Figure 6. (a) Liquid pH, (b) VFAs in the AD process

Table 6. Numerical results of pH and VFAs during the AD process at various $NiCl_2.6H_2O$ doses of 0–8 mg/L

Day	pH					VFAs (mg acetic acid/L)				
	0 mg/L	2 mg/L	4 mg/L	6 mg/L	8 mg/L	0 mg/L	2 mg/L	4 mg/L	6 mg/L	8 mg/L
0	7.03	7.00	7.01	7.03	7.05	2140.23	2140.23	2140.23	2292.01	2140.23
3	6.61	6.54	6.59	6.58	6.55	3567.04	3794.73	3339.36	4553.67	3720.08
6	6.67	6.61	6.69	6.66	6.7	3567.04	3718.83	3111.68	4325.99	3255.07
9	6.6	6.46	6.54	6.81	6.63	3642.94	3794.73	3415.25	4553.67	3642.58
12	6.48	6.34	6.45	6.83	6.52	4022.41	3870.62	3946.51	4705.46	3875.08
15	6.5	6.33	6.36	6.94	6.45	4022.41	3946.51	3720.08	4781.35	3952.59

$NiCl_2.6H_2O$ functions less as a simple additive and more as a process stabilizer, helping to keep hydrolysis, acidogenesis, and methanogenesis in harmony with each other, so that VFAs primarily serve as substrates for methane formation rather than accumulating to inhibitory levels.

Solid removals

The solids removal performance during AD was evaluated by analyzing the removal of TS, TSS, and TDS at various doses of $NiCl_2.6H_2O$ as presented in Figure 7 and Table 7. The results showed that $NiCl_2.6H_2O$ addition had a significant effect on solid reductions, with optimal performance observed at medium concentrations. For TS removal, the control (0 mg/L $NiCl_2.6H_2O$) showed a relatively low removal efficiency of 16.15%. The addition of $NiCl_2.6H_2O$ increased TS removal to 28.57% at a dose of 2 mg/L $NiCl_2.6H_2O$ and reached a maximum of 31.68% at a dose of 4 mg/L $NiCl_2.6H_2O$. However, further increasing the $NiCl_2.6H_2O$ concentration led to a decline in TS removal to 24.34% and 16.15% at doses of 6 and 8 mg/L $NiCl_2.6H_2O$, respectively, indicating inhibitory effects at excessive nickel concentrations. In TSS removal, the removal efficiency increased from 19.35% in the control (0 mg/L $NiCl_2.6H_2O$) to 25.81% at a dose of 2 mg/L $NiCl_2.6H_2O$ and reached a peak of 32.26% at a dose of 4 mg/L $NiCl_2.6H_2O$. At higher doses, TSS removal decreased to 24.05% and 16.13% at doses of 6 and 8 mg/L $NiCl_2.6H_2O$, confirming that excessive nickel addition negatively impacted the degradation of suspended solids. TDS removal also increased with $NiCl_2.6H_2O$. The control (0 mg/L $NiCl_2.6H_2O$) achieved a TDS removal of 13.17%, which increased significantly to 31.14% at doses of 2 and 4 mg/L $NiCl_2.6H_2O$. However, at higher $NiCl_2.6H_2O$ concentrations, TDS removal declined to 24.66% and 16.17% at doses of 6 and 8 mg/L $NiCl_2.6H_2O$, indicating reduced utilization of dissolved organic compounds under inhibitory conditions.

The results demonstrate that $NiCl_2.6H_2O$ addition at concentrations of 2 and 4 mg/L provided the most effective solids removal during AD, while higher doses resulted in diminished performance. Therefore, based on the solids removal performance and the avoidance of inhibitory effects, were conducted using the AD-MEC system at the optimal $NiCl_2.6H_2O$ doses of 2 and 4 mg/L to evaluate the potential of bioelectrochemical enhancement in improving solids degradation and biogas production.

AD vs AD-MEC processes

Biogas production and methane content

In the AD and AD-MEC processes, $NiCl_2.6H_2O$ doses of 2 and 4 mg/L were used. The daily biogas yield is shown in Figure 8(a) and Table 8. The daily biogas yield peak was reached at day 2 for all digesters. The AD-MEC with 2 and 4 mg/L $NiCl_2.6H_2O$ had the daily biogas yield peaks of 253.87 and 103.09 mL/L, respectively. Meanwhile, the AD with 2 and 4 mg/L $NiCl_2.6H_2O$ had the daily biogas yield peaks of 150.78 and 161.55 mL/L, respectively. It means that the AD-MEC with a dose of 2 mg/L $NiCl_2.6H_2O$ demonstrates optimal synergy between biochemical stimulation by Ni and electrochemical activation due to the application of 1.5 V voltage that accelerates hydrolysis and acidogenesis through the enrichment of exoelectrogenic bacteria such as *Geobacter* in the anode biofilm that transfer electrons directly (direct interspecies electron transfer (DIET)) to methanogens and bypass the slow conventional pathway (Indirect Interspecies Electron Transfer – IIET)) (Logan et al., 2019; Yu et al., 2018). At a dose of 2 mg/L $NiCl_2.6H_2O$, Ni serves as

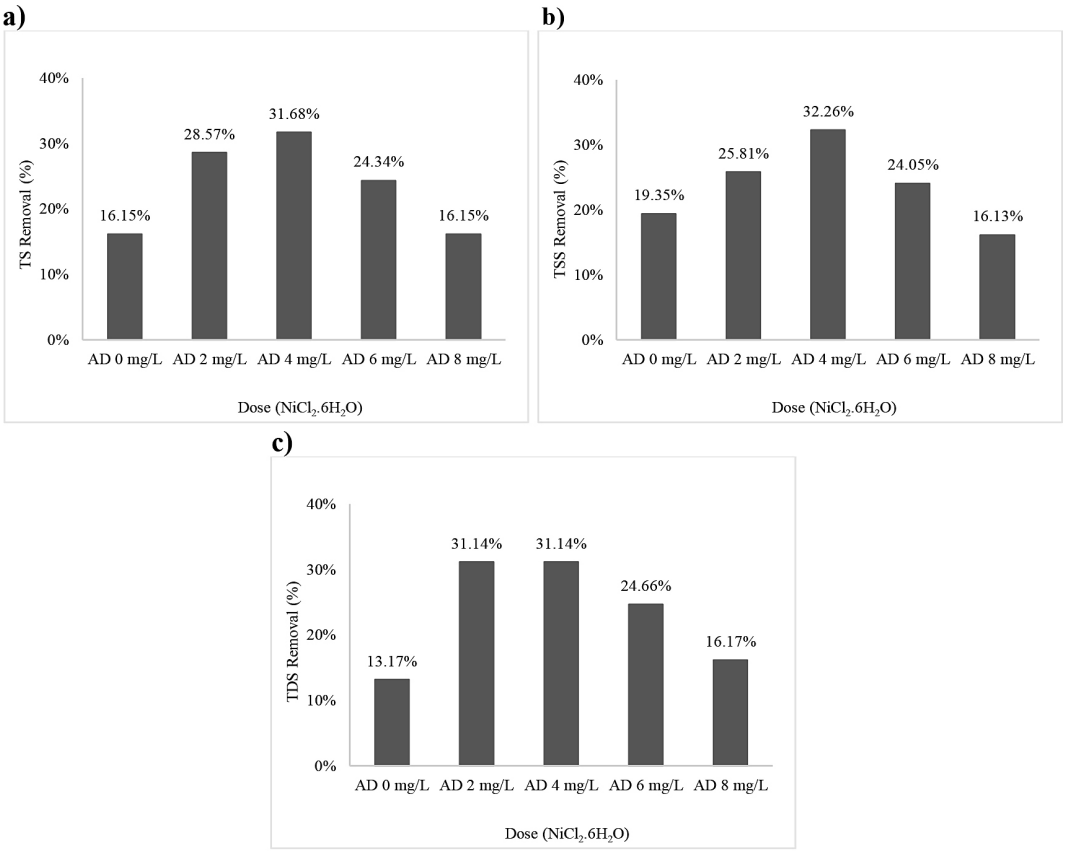

Figure 7. (a) Total solid, (b) total suspended solid, (c) total dissolved solid in the AD process

Table 7. Numerical results of TS, TSS, and TDS during the AD process at various $NiCl_2.6H_2O$ doses of 0–8 mg/L

Parameters	Units	AD				
		0 mg/L	2 mg/L	4 mg/L	6 mg/L	8 mg/L
Initial TS	mg-dry matter/L	16,100	16,100	16,100	15,200	16,100
Final TS	mg-dry matter/L	13,500	11,500	11,000	11,500	13,500
TS removal	%	16.15%	28.57%	31.68%	24.34%	16.15%
Initial TSS	mg-dry matter/L	7,750	7,750	7,750	7,900	7,750
Final TSS	mg-dry matter/L	6,250	5,750	5,250	6,000	6,500
TSS removal	%	19.35%	25.81%	32.26%	24.05%	16.13%
Initial TDS	mg-dry matter/L	8,350	8,350	8,350	7,300	8,350
Final TDS	mg-dry matter/L	7,250	5,750	5,750	5,500	7,000
TDS removal	%	13.17%	31.14%	31.14%	24.66%	16.17%

an essential cofactor for methanogenic enzymes without causing toxic stress, which is thought to allow hydrogenotrophic methanogens to immediately convert H^+ and e^- produced massively at the cathode into methane. This is supported by current measurement data, where the dose of 2 mg/L $NiCl_2.6H_2O$ showed a dynamic current response reaching 29 µA on day 4 and a spike of 54 µA on day 12, indicating intense and sustained biological redox activity. Meanwhile, in AD-MEC with a dose of 4 mg/L $NiCl_2.6H_2O$, the daily biogas yield was much lower and rapidly decreased after day 2, indicating that excess Ni^{2+} in the electroactive environment increased ionic stress and disrupted the stability of the electroactive biofilm. This phenomenon explains why AD-MEC with 4 mg/L $NiCl_2.6H_2O$ was even lower than AD with 4 mg/L, even though in the AD without MEC, the dose of 4 mg/L was actually the optimum dose. In MEC systems, the presence of an electric field narrows

the optimum trace metal dose window. Excess Ni is not only biologically toxic but also disrupts the electrochemical balance at the electrode, suppressing the activity of sensitive microbes, particularly acetoclastic methanogens (Khan et al., 2021). In other words, what is stimulative in AD may not be compatible in an AD-MEC environment due to the additional interactions between metals, biofilms, and electrical currents.

The same pattern was reinforced in the cumulative biogas yield shown in Figure 8(b) and Table 8, where AD-MEC with 2 mg/L $NiCl_2.6H_2O$ produced the highest total biogas yield of 550.82 mL/L, which was 1.6 times higher than conventional AD at the optimum dose (4 mg/L), which confirms the superiority of MEC integration in accelerating methanogenesis activity. This cumulative advantage comes from a combination of several mechanisms namely an increase in the exoelectrogenic bacterial population by more than twofold, which accelerates VFA oxidation at the anode and pH stabilization through proton reduction at the cathode (Wang et al., 2024) and a shift in the methanogenesis pathway from IIET dominance in conventional AD to a combination of DIET+IIET in AD-MEC, which is thermodynamically more efficient (Zhu et al., 2020) as well as the role of Ni as an enzymatic cofactor that maintains high hydrogenase and MCR activities during the active phase (Tian et al., 2016).

Figure 8(b) and Table 8 show that the AD-MEC with 4 mg/L $NiCl_2.6H_2O$ produced the lowest biogas yield, even lower than conventional AD at the same dose. This phenomenon indicates a negative interaction between the external electric field and the Ni^{2+} concentration. In conventional AD, Ni^{2+} is available to microbes through passive diffusion and gradual adsorption into flocs and biofilms, so that at a dose of 4 mg/L, this metal can still act as a trace nutrient that supports methanogenic activity. This condition provides adaptation time for the microbial community. Meanwhile, in the AD-MEC system, the application of an external voltage of 1.5 V changes the electrochemical potential distribution in the digester and increases ion mobility around the electrodes and biofilm. Under these conditions, it is suspected that the presence of Ni^{2+} and Cl^- not only increases conductivity but also accelerates ion accumulation in the active biofilm zone. Consequently, at a dose of 4 mg/L, Ni^{2+}, which is stimulative in conventional AD, turns into a limiting factor in AD-MEC, because the rate of ionic and electrochemical stress exceeds the adaptive capacity of methanogenic microbes. This condition has an impact on acetoclastic methanogens, which are sensitive to environmental changes. Thus, these results strongly indicate that in AD-MEC, the optimum $NiCl_2.6H_2O$ dose shifted to a lower concentration of 2 mg/L compared to the conventional AD with the optimum $NiCl_2.6H_2O$ dose of 4 mg/L, because the success of the system is not only determined by the adequacy of trace metals, but by the complex balance between Ni bioavailability, electric current intensity, electroactive biofilm stability, and microbial electron transfer pathways.

The methane content in biogas was analyzed and shown in Table 9. Furthermore, the daily and cumulative methane yields (mL-CH_4/L) were calculated and shown in Figure 9(a) and Figure 9(b), respectively. The numerical results are shown in Table 10. The daily methane yield profile shown in Figure 9(a) and Table 10 shows that $NiCl_2.6H_2O$

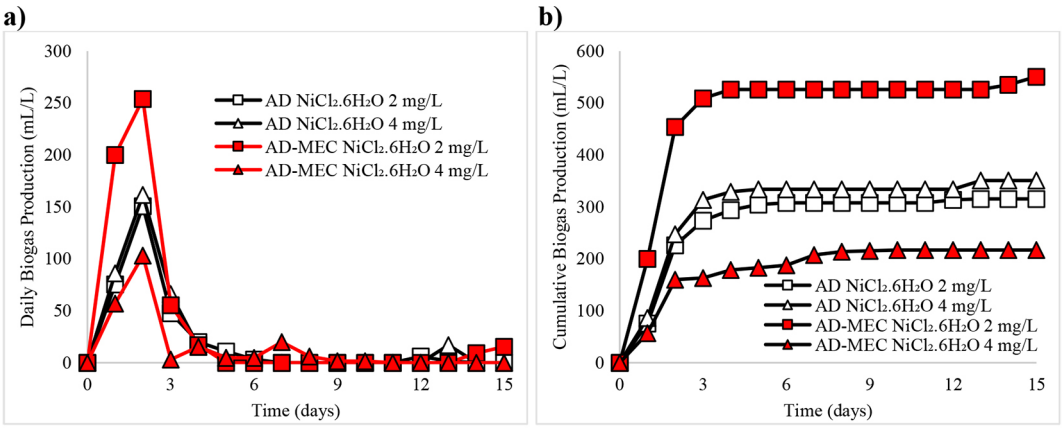

Figure 8. (a) Daily biogas yield, (b) cumulative biogas yield in the AD and AD-MEC processes

Table 8. Numerical results of daily and cumulative biogas yield during AD and AD-MEC processes at various $NiCl_2.6H_2O$ doses of 2–4 mg/L

Day	Daily biogas yield (mL/L)				Cumulative biogas yield (mL/L)			
	AD 2 mg/L	AD 4 mg/L	AD-MEC 2 mg/L	AD-MEC 4 mg/L	AD 2 mg/L	AD 4 mg/L	AD-MEC 2 mg/L	AD-MEC 4 mg/L
0	0.00	0.00	0.00	0.00	0.00	0.00	0.00	0.00
1	75.39	86.16	200.02	56.93	75.39	86.16	200.02	56.93
2	150.78	161.55	253.87	103.09	226.17	247.71	453.89	160.01
3	47.70	66.16	55.39	3.08	273.87	313.87	509.28	163.09
4	20.00	15.39	16.92	15.39	293.87	329.26	526.20	178.48
5	10.77	4.62	0.00	4.62	304.64	333.88	526.20	183.09
6	3.08	0.00	0.00	4.62	307.72	333.88	526.20	187.71
7	0.00	0.00	0.00	20.00	307.72	333.88	526.20	207.71
8	0.00	0.00	0.00	6.15	307.72	333.88	526.20	213.87
9	0.00	0.00	0.00	1.54	307.72	333.88	526.20	215.40
10	0.00	0.00	0.00	1.54	307.72	333.88	526.20	216.94
11	0.00	0.00	0.00	0.00	307.72	333.88	526.20	216.94
12	6.15	0.00	0.00	0.00	313.87	333.88	526.20	216.94
13	1.54	16.92	0.00	0.00	315.41	350.80	526.20	216.94
14	0.00	0.00	9.23	0.00	315.41	350.80	535.43	216.94
15	0.00	0.00	15.39	0.00	315.41	350.80	550.82	216.94

supplementation accelerates the initial phase of methanogenesis, but the response is highly dependent on the process configuration. In conventional AD, the peak methane yield occurred on day 2, with the highest value at a dose of 4 mg/L of 135.78 mL-CH_4/L, slightly higher than the 126.56 mL-CH_4/L dose at 2 mg/L. This indicates that in a system without an electric field, increasing Ni^{2+} availability to 4 mg/L is still within the stimulative range, especially in the initial phase when readily degradable substrates are still abundant. Ni acts as an enzymatic cofactor in various methanogenic metalloenzymes, thereby increasing the conversion rate to CH_4. This is because the addition of nickel to the digester increases the production of methyl-coenzyme M-reductase (MCR) and accelerates the methanogenic phase. Other gases, such as CO_2 and H_2, are consumed to produce more methane (Tian et al., 2016). However, after the 3rd day, methane yield at both AD doses decreased sharply, indicating the system's limitations in maintaining methanogenic activity when the easily decomposable carbon fraction has been depleted, and nitrogen pressure begins to increase, considering the character of TILW, which has a low C/N ratio. Meanwhile, in the AD-MEC system with a dose of 2 mg/L $NiCl_2.6H_2O$, the peak daily methane yield was reached on the 2nd day at 182.73 mL-CH_4/L, which had already shown high production since the 1st day at 143.97 mL-CH_4/L. This spike indicates that the combination of bioavailable Ni^{2+} and an external electric field effectively accelerates electron transfer and methanogen activation, especially the hydrogenotrophic pathway. The application of a voltage of 1.5 V to MEC-AD triggers a shift in the metabolic pathway from IIET to DIET via *Geobacter* (Logan et al., 2019; Yu et al., 2018). This DIET pathway is more resistant to ammonia inhibition and is able to transfer electrons directly to hydrogenotrophic methanogens to reduce CO_2 to methane. It acts as an essential cofactor in hydrogenase and methyl-coenzyme M reductase enzymes, thereby accelerating the conversion of H_2/CO_2 to CH_4 (Khan et al., 2021). The sharp decrease in methane yield after day 4 in all systems reflects the characteristics of TILW, which has a low C/N ratio and high nitrogen content, making carbon readily degradable at the beginning, while the accumulation of nitrogen, mainly in the form of free ammonia, begins to suppress methanogenic activity in the later phase.

In the cumulative methane yields shown in Figure 9(b) and Table 10, at the end of the observation, namely the 15th day, AD with a dose of 4 mg/L $NiCl_2.6H_2O$ produced the highest cumulative methane among the AD systems, namely 294.84 mL-CH_4/L, greater than AD 2 mg/L of 264.74 mL-CH_4/L. This indicates that

in conventional AD, a slightly higher Ni dose is able to maintain methanogenic activity. However, this performance is still far behind the AD-MEC 2 mg/L, which achieved a cumulative methane of 396.48 mL-CH_4/L, or about 1.3 times higher than AD with a dose of 4 mg/L $NiCl_2.6H_2O$. The superiority of AD-MEC comes not only from the initial peak production but also from the system's ability to maintain methane accumulation even though the substrate conditions are less than ideal. In TILW with a low C/N ratio and high nitrogen content, conventional AD quickly experiences redox imbalance due to the limitation of organic electron donors. The integration of AD-MEC essentially opens an additional electron supply pathway from the cathode that can be directly utilized by hydrogenotrophic methanogens, allowing CO_2 reduction to CH_4 to continue even as dissolved carbon in the substrate begins to decline. Therefore, methane production in AD-MEC continues to increase until the end of the period, whereas in conventional AD, the methane formation rate slows rapidly and the system reaches saturation more quickly. The suboptimal performance of AD at a dose of 4 mg/L $NiCl_2 \cdot 6H_2O$ also indicates that, without the aid of an electrochemical field, higher Ni additions do not automatically increase methane production and can even potentially cause metal stress and disrupt the balance of the microbial community (Khan et al., 2021). These findings indicate that the combination of trace metal Ni with AD-MEC technology works simultaneously to improve electron transfer and methanogenesis efficiency on substrates with low C/N ratios, making the AD-MEC configuration at 2 mg/L $NiCl_2 \cdot 6H_2O$ the most reasonable choice in terms of process kinetics, microbial stability, and system energy performance.

Table 9 shows that the percentage of methane content in biogas from the conventional AD process with the addition of $NiCl_2 \cdot 6H_2O$ was relatively higher than that of the AD-MEC system. However, when viewed in absolute terms, the AD-MEC system still produced a larger total methane volume because its overall biogas production was indeed higher. At AD with 2 and 4 mg/L $NiCl_2.6H_2O$, CH_4 contents reached 83.9% and 84.0%, respectively, indicating that the methanogenesis pathway runs very efficiently and selectively towards methane formation when bioavailable Ni is in the optimal range. This is in line with the role of Ni as a major cofactor of methyl-coenzyme M reductase, so that most of the biogas formed is directly converted to CH_4 without accumulation of intermediate gases. The AD-MEC with 2 mg/L $NiCl_2.6H_2O$ showed a lower CH_4 percentage of 72.0%, but produced the highest daily and cumulative methane yields. This phenomenon reflects the unique characteristics of the MEC system, where the increase in total gas and electron flow at the cathode leads to greater absolute methane production, but with a more heterogeneous biogas composition. In AD-MEC, some electrons are channeled through hydrogenotrophic and electrochemical pathways

Table 9. Methane content in AD and AD-MEC processes

Sample	CH_4 content (%)*
AD $NiCl_2.6H_2O$ 2 mg/L	83.9
AD $NiCl_2.6H_2O$ 4 mg/L	84.0
AD-MEC $NiCl_2.6H_2O$ 2 mg/L	72.0

Note: *measured on day 3 and assumed as the average value.

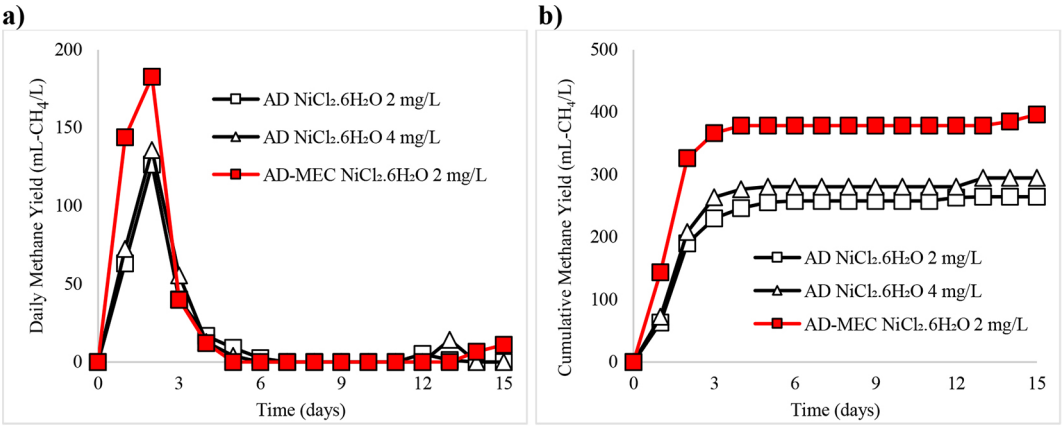

Figure 9. (a) Daily methane yield, (b) cumulative methane yield in the AD and AD-MEC processes

Table 10. Numerical results of daily and cumulative methane yield during the AD and AD-MEC processes at various $NiCl_2.6H_2O$ doses of 2–4 mg/L

Day	Daily methane yield (mL-CH_4/L)			Cumulative methane yield (mL-CH_4/L)		
	AD 2 mg/L	AD 4 mg/L	AD-MEC 2 mg/L	AD 2 mg/L	AD 4 mg/L	AD-MEC 2 mg/L
0	0.00	0.00	0.00	0.00	0.00	0.00
1	63.28	72.42	143.97	63.28	72.42	143.97
2	126.56	135.78	182.73	189.84	208.20	326.71
3	40.03	55.61	39.87	229.88	263.80	366.58
4	16.79	12.93	12.18	246.66	276.74	378.76
5	9.04	3.88	0.00	255.70	280.62	378.76
6	2.58	0.00	0.00	258.29	280.62	378.76
7	0.00	0.00	0.00	258.29	280.62	378.76
8	0.00	0.00	0.00	258.29	280.62	378.76
9	0.00	0.00	0.00	258.29	280.62	378.76
10	0.00	0.00	0.00	258.29	280.62	378.76
11	0.00	0.00	0.00	258.29	280.62	378.76
12	5.17	0.00	0.00	263.45	280.62	378.76
13	1.29	14.22	0.00	264.74	294.84	378.76
14	0.00	0.00	6.64	264.74	294.84	385.40
15	0.00	0.00	11.07	264.74	294.84	396.48

that increase the total gas volume so that the CH_4 fraction is relatively decreased even though the pure CH_4 volume increases significantly. In other words, AD emphasizes the quality of CH_4 gas, while AD-MEC emphasizes the quantity of absolute methane yield. This relationship emphasizes that the process is not only based on the percentage of CH_4, but considers the actual methane yield, which in the AD-MEC system is superior for clean energy utilization from TILW.

Liquid pH and volatile fatty acids (VFAs)

The pH profiles of the liquids in Figure 10(a) and Table 11 show a clear difference in system behavior between conventional AD and AD-MEC at the same $NiCl_2.6H_2O$ doses. In all treatments, the initial pH was in the neutral range, then decreased sharply until day 3 due to the dominance of the acidogenesis phase. However, the AD-MEC system with 2 mg/L $NiCl_2.6H_2O$ showed the most stable and highest pH recovery, increasing gradually from 6.48 on day 3 to 6.86 on day 15, surpassing all other AD and AD-MEC variations. In contrast, at AD with 2 and 4 mg/L $NiCl_2.6H_2O$, the pH continued to decrease to a range of 6.33–6.36 at the end of operation, indicating that VFA consumption by methanogens was unable to keep up with their formation rate.

This superiority of AD-MEC with 2 mg/L $NiCl_2.6H_2O$ was due to the synergy between the supply of Ni as a functional trace element and the activation of electron transfer by the electric field, which accelerated the transition from acidogenesis to methanogenesis. Furthermore, Ni is an essential component of the low-molecular-weight coenzyme F_{430}, which utilizes two coenzymes, methyl thio-ether-methyl-coenzyme M and coenzyme thiol B, as substrates for methane production in all methanogens. Ni has also been reported to directly promote acidogenesis rather than methanogenesis, thereby promoting VFA production (Khan et al., 2021; Tsapekos et al., 2018). The presence of Ni acts as a cofactor for the urease enzyme, which is crucial in degrading the high protein content in TILW. In TILW substrates that are poor in carbohydrates but rich in nitrogen, ammonia formation is relatively high, so that the system has a better buffer capacity than carbohydrate-rich substrates. This condition allows AD-MEC to utilize excess total ammonia nitrogen (TAN) to withstand pH decreases while maintaining methanogenic activity. At a $NiCl_2.6H_2O$ dose of 4 mg/L, both in AD and AD-MEC, the pH tends to be lower and stable, indicating that increasing ion concentrations Ni^{2+} and Cl^- begin to shift the osmotic and metabolic balance of microbes so that the kinetic benefits of Ni addition are no longer linear.

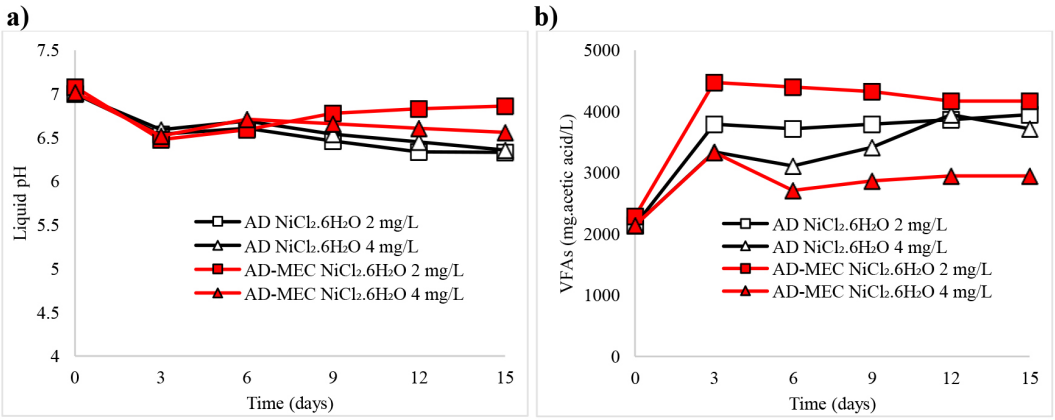

Figure 10. (a) Liquid pH (b) volatile fatty acids (VFAs) in the AD and AD-MEC processes

Table 11. Numerical results of pH and VFAs during the AD and AD-MEC processes at various $NiCl_2.6H_2O$ doses of 2–4 mg/L

Day	pH				VFAs (mg acetic acid/L)			
	AD 2 mg/L	AD 4 mg/L	AD-MEC 2 mg/L	AD-MEC 4 mg/L	AD 2 mg/L	AD 4 mg/L	AD-MEC 2 mg/L	AD-MEC 4 mg/L
0	7	7.01	7.08	7.02	2140.23	2140.23	2292.01	2140.23
3	6.54	6.59	6.48	6.52	3794.73	3339.36	4477.78	3332.57
6	6.61	6.69	6.59	6.71	3718.83	3111.68	4401.88	2712.56
9	6.46	6.54	6.78	6.66	3794.73	3415.25	4325.99	2867.56
12	6.34	6.45	6.83	6.61	3870.62	3946.51	4174.20	2945.06
15	6.33	6.36	6.86	6.56	3946.51	3720.08	4174.20	2945.06

In the VFA profile shown in Figure 10(b) and Table 11, the highest VFA accumulation occurred in AD-MEC with 2 mg/L $NiCl_2.6H_2O$, reaching 4174.20 mg acetic acid/L, followed by AD with 2 mg/L $NiCl_2.6H_2O$, AD with 4 mg/L $NiCl_2.6H_2O$, and the lowest in AD-MEC with 4 mg/L $NiCl_2.6H_2O$. The high VFA concentration in AD-MEC with 2 mg/L $NiCl_2.6H_2O$ does not indicate process failure, but rather reflects highly active hydrolysis and acidogenesis, accelerated by the presence of electrogenic microorganisms and direct electron transfer pathways that enhance the conversion of TILW substrates into volatile acids. In contrast to conventional AD, VFA accumulation in AD-MEC is not followed by an excessive decrease in pH because VFA consumption by methanogens is more efficient, so that the system remains in the optimal pH zone, which ranges from 6.48–6.86. On the opposite side, in AD-MEC with 4 mg/L $NiCl_2.6H_2O$, the VFA concentration was the lowest, indicating an obstacle in the early stages of fermentation, due to the ionic pressure of Cl^- and excess Ni, which reduced the activity of hydrolytic and acidogenic bacteria before optimal VFA formation. The combination of an electrical current and a 4 mg/L $NiCl_2.6H_2O$ dose created an environment that began to be toxic, so that organic substrates were not broken down into VFAs. In conventional AD, the more intermediate VFA pattern, but followed by a decrease in pH, indicated that the conversion of VFAs to methane was slower and highly dependent on the TAN-alkalinity balance, which in TILW is fluctuating. The combination of 2 mg/L $NiCl_2.6H_2O$ and AD-MEC created a more resilient reaction condition to pH-VFA fluctuations than conventional AD.

Solids removals

The comparison of solids removal performance between the AD and AD-MEC systems at the selected optimal $NiCl_2.6H_2O$ doses of 2 and 4 mg/L is presented in Figure 11 and Table 12.

At 2 mg/L $NiCl_2.6H_2O$, the AD-MEC system consistently outperformed the conventional AD process. TS removal increased from 28.57% in AD to 37.50% in AD-MEC, while TSS removal showed a more pronounced improvement from 25.81% to 39.87%. TDS removal also increased

from 31.14% in AD to 34.93% under AD-MEC conditions, showing enhanced degradation of both suspended and dissolved solids. At a dose of 4 mg/L $NiCl_2.6H_2O$, the AD-MEC system showed lower solid removal efficiency than the AD system. TS removal decreased from 31.68% in AD to 22.36% in AD-MEC, while TSS and TDS removals decreased from 32.26% and 31.14% to 22.58% and 22.16%, respectively. These results suggest that the beneficial effect of MEC integration on solid removal was more evident at the lower $NiCl_2.6H_2O$ dose. The findings indicate that AD-MEC with 2 mg/L $NiCl_2.6H_2O$ provided the most favorable condition for solids removal, consistent with the enhanced biogas production observed in this study.

Kinetic analysis

The kinetic constants estimated using the modified Gompertz model clearly indicate that both the concentration of $NiCl_2.6H_2O$ and the type of reactor configuration play an important role in shaping the biogas production performance. As shown in Table 13 and Figure 12.

The model accurately described the experimental results as indicated by consistently high R^2 values (0.9948-0.9986) along with low SSE, and showed that the cumulative biogas profiles from the AD and AD-MEC systems follow the expected microbial growth-based kinetic patterns. In the AD system, the maximum biogas potential (P_m) increased from 166.00 mL/L at 0 mg/L $NiCl_2.6H_2O$ (control) to 309.30 mL/L at 2 mg/L $NiCl_2.6H_2O$ and reached a maximum of 383.39 mL/L at 4 mg/L $NiCl_2.6H_2O$. However, further increases in $NiCl_2.6H_2O$ concentration led to a decrease in (P_m to 297.82 mL/L and 124.41 mL/L at 6 and 8 mg/L $NiCl_2.6H_2O$, respectively, indicating inhibitory effects at excessive nickel levels. A similar trend was observed for the maximum biogas production rate (μ), which increased from 141.03 mL/L/day at 0 mg/L (control) to 184.25 mL/L/day at 4 mg/L $NiCl_2.6H_2O$, before declining sharply at higher concentrations.

Compared to conventional AD, the AD-MEC system exhibited substantially higher kinetic parameters. At 2 mg/L $NiCl_2.6H_2O$, AD-MEC had (P_m value of 528.89 mL/L, which was higher than the (P_m obtained in the AD system (309.30 mL

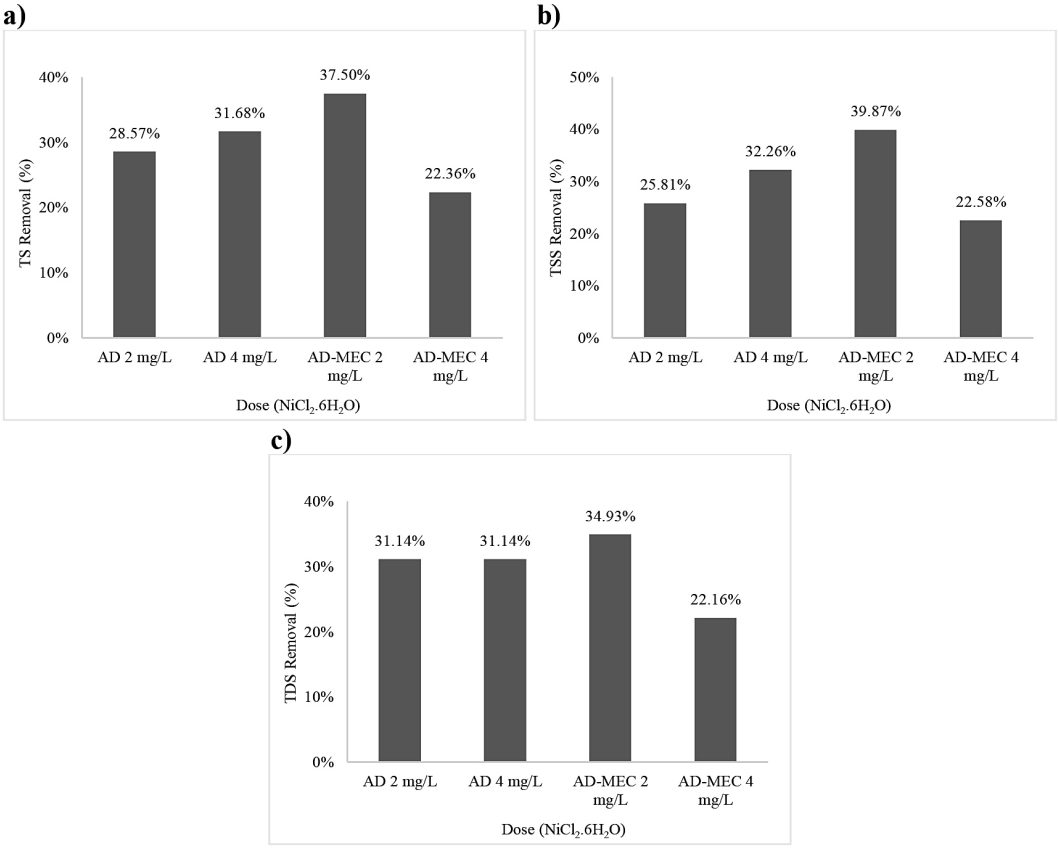

Figure 11. (a) Total solid, (b) total suspended solid, (c) total dissolved solid in the AD and AD-MEC processes

Table 12. Numerical results of TS, TSS, and TDS during the AD and AD-MEC processes at various $NiCl_2.6H_2O$ doses of 2–4 mg/L

Parameters	Units	AD		AD-MEC	
		2 mg/L	4 mg/L	2 mg/L	4 mg/L
Initial TS	mg-dry matter/L	16,100	16,100	15,200	16,100
Final TS	mg-dry matter/L	11,500	11,000	9,500	12,500
TS removal	%	28.57%	31.68%	37.50%	22.36%
Initial TSS	mg-dry matter/L	7,750	7,750	7,900	7,750
Final TSS	mg-dry matter/L	5,750	5,250	4,750	6,000
TSS removal	%	25.81%	32.26%	39.87%	22.58%
Initial TDS	mg-dry matter/L	8,350	8,350	7,300	8,350
Final TDS	mg-dry matter/L	5,750	5,750	4,750	6,500
TDS removal	%	31.14%	31.14%	34.93%	22.16%

Table 13. Kinetic constant values

Constants	Unit	AD					AD-MEC	
		$NiCl_2.6H_2O$ 0 mg/L	$NiCl_2.6H_2O$ 2 mg/L	$NiCl_2.6H_2O$ 4 mg/L	$NiCl_2.6H_2O$ 6 mg/L	$NiCl_2.6H_2O$ 8 mg/L	$NiCl_2.6H_2O$ 2 mg/L	$NiCl_2.6H_2O$ 4 mg/L
P_m	mL/L	166.00	309.30	338.39	299.82	124.41	528.89	210.24
μ	mL/L/day	141.03	155.11	181.48	257.46	53.66	353.34	69.96
λ	days	0.77	0.50	0.53	0.48	0.76	0.43	0.07
P_m (experiment)	mL/L	167.71	315.41	350.80	304.64	124.63	550.82	216.94
SSE	-	56.2	386.0	625.5	538.07	96.51	632.27	2558.95
R^2	-	0.9986	0.9971	0.9961	0.9948	0.9961	0.9982	0.9980

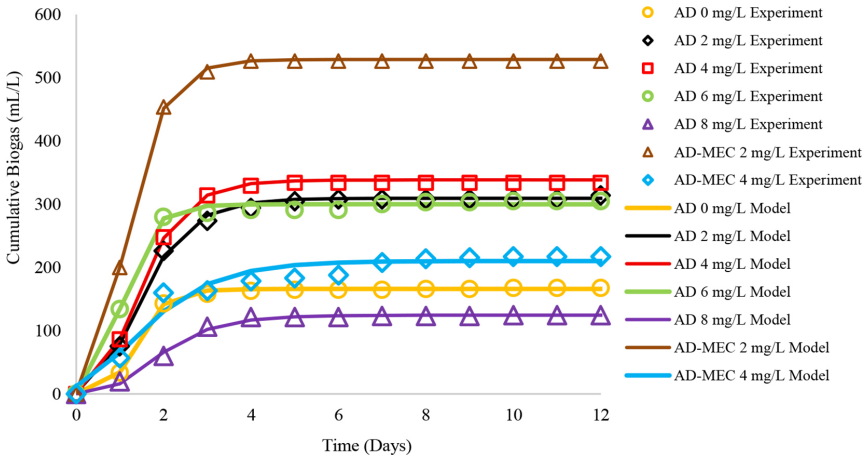

Figure 12. Plotting results using the modified Gompertz model

/L). The corresponding μ value also increased significantly, reaching 353.34 mL/L/day at 2 mg/L $NiCl_2.6H_2O$, indicating a much faster biogas production rate under AD-MEC than that under AD. The lag phase (λ) further highlights the improved performance of the AD-MEC system. At 2 mg/L $NiCl_2.6H_2O$, the AD had a longer lag phase (0.50 days), whereas the AD-MEC shortened the lag phase to 0.43 days, indicating rapid microbial adaptation. The kinetic analysis confirms that the optimum conditions were AD-MEC with a dose of 2 mg/L $NiCl_2.6H_2O$. The addition of $NiCl_2.6H_2O$ and integration with MEC significantly improved both the biogas yield and production rate.

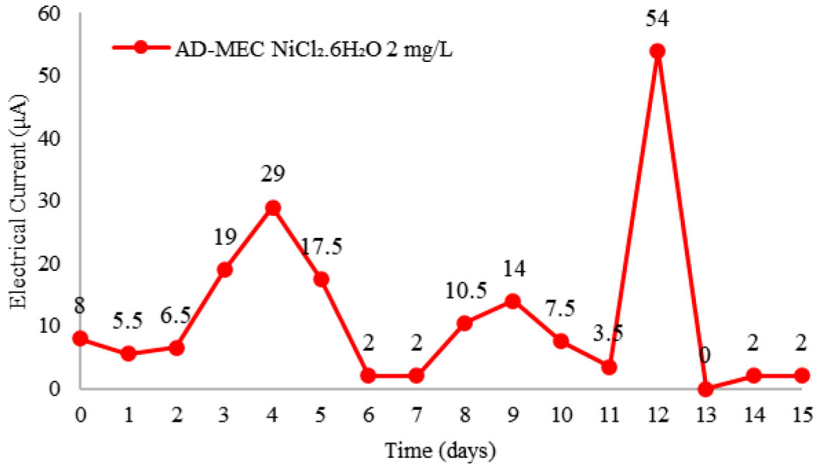

Figure 13. Electrical current during AD-MEC with $NiCl_2.6H_2O$ 2 mg/L

Table 14. Energy analysis values

Parameters	AD $NiCl_2.6H_2O$ 4 mg/L	AD-MEC $NiCl_2.6H_2O$ 2 mg/L
Voltage (V)	0	1.5 V
Average current (A)	0	1.14×10^{-5}
Time (s)	1296000	1296000
Input energy (J)	0	22.23
Methane yield (mL-CH_4/L)	294.84	396.48
Methane volume (L)	0.118	0.159
Output energy (J)	2928.50	3938.02
Surplus energy (J)	2928.50	3915.79

Energy analysis

Energy analysis was conducted to assess the feasibility of MEC in AD. In this analysis, the optimal condition for AD was compared with the optimal condition for AD-MEC, namely AD with $NiCl_2.6H_2O$ 4 mg/L and AD-MEC with $NiCl_2.6H_2O$ 2 mg/L. The energy analysis was conducted by following the formula used by Syaichurrozi et al. (2024). The profile of electrical current during AD-MEC with $NiCl_2.6H_2O$ 2 mg/L is shown in Figure 13.

In the conventional AD system, no external electrical energy was supplied. Therefore, the energy input was zero. Under these conditions, the AD system produced an energy output of 2928.50 J, which was derived entirely from methane production. The AD-MEC system required a small electrical energy input of 22.23 J to maintain an applied voltage of 1.5 V. Despite this additional energy requirement, the integration of MEC substantially improved methane recovery, which was resulting in a higher energy output of 3938.02 J. Detailed calculation is shown in Table 14.

After accounting for electricity consumption, the net energy surplus of the AD-MEC system reached 3915.79 J, which is 34% higher or 1.3 times higher than that of the conventional AD system. These results showed that MEC significantly improved net energy recovery, even after accounting for electricity consumption. The larger energy surplus observed in the AD-MEC system stems primarily from higher methane production, indicating that the overall methane volume was the primary driver of the energy balance. In other words, the electrical power required to run the MEC was easily offset by the additional methane produced, making the AD-MEC configuration energetically advantageous and strengthening its potential as a clean energy generation option for TILW treatment.

CONCLUSIONS

The optimum $NiCl_2.6H_2O$ dose in the AD process was 4 mg/L, while in the AD-MEC process was 2 mg/L. Therefore, the AD-MEC with 2 mg/L

$NiCl_2.6H_2O$ showed the most favorable results, achieving the highest daily biogas yield of 253.87 mL/L on day 2 and the highest cumulative biogas yield of 550.82 mL/L, approximately 1.6 times higher than conventional AD at the optimum dose (4 mg/L). In addition, the AD-MEC with 2 mg/L $NiCl_2.6H_2O$ generated the cumulative methane yield of 396.48 mL-CH_4/L, exceeding AD with 4 mg/L $NiCl_2.6H_2O$. The AD-MEC with 2 mg/L $NiCl_2.6H_2O$ also resulted in the highest TS, TSS, and TDS removals, namely 37.50%, 39.87%, and 34.93%, respectively. Energy analysis revealed that AD-MEC with 2 mg/L $NiCl_2.6H_2O$ produced a surplus energy of 3915.79 J, which was 34% or 1.3 times higher than conventional AD with 4 mg/L $NiCl_2.6H_2O$ (2928.50 J). The research results are in accordance with the hypothesis that appropriate Ni dosing significantly enhances biogas and methane yields, with a more pronounced effect observed in the AD-MEC process.

REFERENCES

1. Abdelsalam, E., Samer, M., Abdel-Hadi, M. A., Hassan, H. E., Badr, Y. (2015). Effect of $COCl_2$, $NiCl_2$ and $FeCl_3$ additives on biogas and methane production. *Misr Journal of Agricultural Engineering*, *32*(2), 843–862. https://doi.org/10.21608/mjae.2015.98656
2. Alharbi, M., Alkathami, B. S. (2024). Modeling of biogas production of camel and sheep manure using tomato and rumen as co-substrate via kinetic models. *Journal of Ecological Engineering*, *25*(8), 10–23. https://doi.org/10.12911/22998993/189231
3. Arifan, F., Abdullah, A., Sumardiono, S. (2021). Effect of organic waste addition into animal manure on biogas production using anaerobic digestion method. *International Journal of Renewable Energy Development*, *10*(3), 623–633. https://doi.org/10.14710/ijred.2021.36107
4. Fermoso, F. G., Bartacek, J., Jansen, S., Lens, P. N. L. (2009). Metal supplementation to UASB bioreactors: from cell-metal interactions to full-scale application. *Science of the Total Environment*, *407*(12), 3652–3667. https://doi.org/10.1016/j.scitotenv.2008.10.043
5. Huwaida, A. F., Nurpadhilah, A. D., Budiastuti, H., Ramadhani, L. I. (2024). The evaluation of seeding process of tofu wastewater treatment in anaerobic sequencing batch reactor. *AIP Conference Proceedings*, *030002*(March 2019). https://doi.org/https://doi.org/10.1063/5.0181560
6. Khan, S., Lu, F., Kashif, M., Shen, P. (2021). Multiple effects of different nickel concentrations on the stability of anaerobic digestion of molasses. *Sustainability (Switzerland)*, *13*(9). https://doi.org/10.3390/su13094971
7. Khomariah, N., Syaichurrozi, I., Kurniawan, T., Sulaiman, F., Ridwan, A., Budiyono, Hashim, H. (2025). Impact of feed pH on biogas generation from liquid waste of tapioca starch industry through anaerobic digestion assisted by microbial electrolysis cell. *Journal of Ecological Engineering*, *26*(12), 291–303. https://doi.org/10.12911/22998993/207796
8. Logan, B. E., Rossi, R., Ragab, A., Saikaly, P. E. (2019). Electroactive microorganisms in bioelectrochemical systems. *Nature Reviews | Microbiology*, *1*. https://doi.org/10.1038/s41579-019-0173-x
9. Matheri, A. N., Belaid, M. (2016). The role of trace elements on anaerobic co-digestion in biogas production. *Newswood Limited*, *II*, 784–789.
10. Neubeck, A., Sjoberg, S., Price, A., Callac, N., Schnurer, A. (2016). Effect of nickel levels on hydrogen partial pressure and methane production in methanogens. *Plos One*, *11*(12), 1–19. https://doi.org/10.1371/journal.pone.0168357
11. Osazuwa, E. O. (2022). Effect of nickel chloride on the production of biogas from cow dung. *European of Biomedical AND Pharmaceutical Sciences*, *9*(2), 50–52.
12. Paulo, L. M., Ramiro-Garcia, J., van Mourik, S., Stams, A. J. M., Sousa, D. Z. (2017). Effect of nickel and cobalt on methanogenic enrichment cultures and role of biogenic sulfide in metal toxicity attenuation. *Frontiers in Microbiology*, *8*(JUL), 1–12. https://doi.org/10.3389/fmicb.2017.01341
13. Rahmat, B., Hartoyo, T., Sunarya, Y. (2014). Biogas production from tofu liquid waste on treated agricultural wastes. *American Journal of Agricultural and Biological Science*, *9*(2), 226–231. https://doi.org/10.3844/ajabssp.2014.226.231
14. Ramadhani, L. I., Nabila, S. A., Angela, S., Budiastuti, H. (2025). Enhancing tofu wastewater treatment efficiency with water hyacinth extract addition in an anaerobic sequencing batch reactor. *Fluida*, *18*(1), 38–45. https://doi.org/10.35313/fluida.v18i1.6164
15. Syaichurrozi, I., Murtiningsih, I., Angelica, E. C., Susanti, D. Y., Raharjo, J., Timuda, G. E., Darsono, N., Primeia, S., Suwandi, E., Kurniawan, Khaerudini, D. S. (2024). A preliminary study: Microbial electrolysis cell assisted anaerobic digestion for biogas production from Indonesian tofu-processing wastewater at various Fe additions. *Renewable Energy*, *234*(August), 121203. https://doi.org/10.1016/j.renene.2024.121203
16. Syaichurrozi, I., Nurulshani, S., Pramudita, A. A., Suhendi, E., Kustiningsih, I., Darsono, N., Khaerudini, D. S. (2025). Biogas generation from anaerobic co-digestion of tofu liquid waste and tapioca flour liquid waste at various initial pHs. *Journal of Ecological Engineering*, *26*(7), 11–23. https://doi.org/10.12911/22998993/202913

17. Takashima, M., Shimada, K., Speece, R. E. (2011). Minimum requirements for trace metals (Iron, Nickel, Cobalt, and Zinc) in thermophilic and mesophilic methane fermentation from glucose. *Water Environment Research*, *83*(4), 339–346. https://doi.org/10.2175/106143010x12780288628895
18. Tian, Y., Zhang, H., Chai, Y., Wang, L., Mi, X., Zhang, L., Adam, M. (2016). Biogas properties and enzymatic analysis during anaerobic fermentation of phragmites australis straw and cow dung : influence of nickel chloride supplement. *Biodegradation*. https://doi.org/10.1007/s10532-016-9774-5
19. Tsapekos, P., Alvarado-Morales, M., Tong, J., Angelidaki, I. (2018). Nickel spiking to improve the methane yield of sewage sludge. *Bioresource Technology*, *270*, 732–737. https://doi.org/10.1016/j.biortech.2018.09.136
20. Wang, D., Hao, Z., Tao, S., Shi, Z., Liu, Z., Liu, E., Long, S. (2024). Enhanced methane production from waste activated sludge by microbial electrolysis cell assisted anaerobic digestion: Fate and effect of humic substances. *Bioresource Technology*, *403*(March), 130872. https://doi.org/10.1016/j.biortech.2024.130872
21. Xu, X. J., Wang, W. Q., Chen, C., Xie, P., Liu, W. Z., Zhou, X., Wang, X. T., Yuan, Y., Wang, A. J., Lee, D. J., Yuan, Y. X., Ren, N. Q. (2020). The effect of PBS on methane production in combined MEC-AD system fed with alkaline pretreated sewage sludge. *Renewable Energy*, *152*, 229–236. https://doi.org/10.1016/j.renene.2020.01.052
22. Yu, Z., Leng, X., Zhao, S., Ji, J., Zhou, T., Khan, A., Kakde, A., Liu, P., Li, X. (2018). A review on the applications of microbial electrolysis cells in anaerobic digestion. *Bioresource Technology*, *255*(November 2017), 340–348. https://doi.org/10.1016/j.biortech.2018.02.003
23. Zhu, X., Zhou, P., Chen, Y., Liu, X., Li, D. (2020). The role of endogenous and exogenous hydrogen in the microbiology of biogas production systems. *World Journal of Microbiology and Biotechnology*, *36*(6), 1–7. https://doi.org/10.1007/s11274-020-02856-9
24. Zwietering, M. H., Jongenburger, I., Rombouts, F. M., Van't Riet, K. (1990). Modeling of the bacterial growth curve. *Applied and Environmental Microbiology*, *56*(6), 1875–1881. https://doi.org/10.1128/aem.56.6.1875-1881.1990